

1 Comparative geochemical study on Furongian–earliest Ordovician (Toledanian)
2 and Ordovician (Sardic) felsic magmatic events in south-western Europe:
3 underplating of hot mafic magmas linked to the opening of the Rheic Ocean

4

5 J. Javier Álvaro^{a*}, Teresa Sánchez-García^b, Claudia Puddu^c, Josep Maria Casas^d,
6 Alejandro Díez-Montes^e, Montserrat Liesa^f & Giacomo Oggiano^g

7

8 ^a *Instituto de Geociencias (CSIC-UCM), Dr. Severo Ochoa 7, 28040 Madrid, Spain,*
9 *jj.alvaro@csic.es*

10 ^b *Instituto Geológico y Minero de España, Ríos Rosas 23, 28003 Madrid, Spain,*
11 *t.sanchez@igme.es*

12 ^c *Dpto. Ciencias de la Tierra, Universidad de Zaragoza, 50009 Zaragoza, Spain,*
13 *claudiapuddugeo@gmail.com*

14 ^d *Dpt. de Dinàmica de la Terra i de l'Oceà, Universitat de Barcelona, Martí Franquès*
15 *s/n, 08028 Barcelona, Spain, casas@ub.edu*

16 ^e *Instituto Geológico y Minero de España, Plaza de la Constitución 1, 37001*
17 *Salamanca, Spain, al.diez@igme.es*

18 ^f *Dept. de Mineralogia, Petrologia i Geologia aplicada, Universitat de Barcelona, Martí*
19 *Franquès s/n, 08028 Barcelona, Spain, mliesa@ub.edu*

20 ^g *Dipartimento di Scienze della Natura e del Territorio, 07100 Sassari, Italy,*
21 *giacoggi@uniss.it*

22

23 * Corresponding author

24

25 **ABSTRACT**

26

27 A geochemical comparison of Early Palaeozoic felsic magmatic episodes throughout
28 the south-western European margin of Gondwana is made, and includes (i) Furongian–
29 Early Ordovician (Toledanian) activities recorded in the Central Iberian and Galicia-Trás-
30 os-Montes Zones of the Iberian Massif, and (ii) Early–Late Ordovician (Sardic) activities
31 in the eastern Pyrenees, Occitan Domain (Albigeois, Montagne Noire and Mouthoumet
32 massifs) and Sardinia. Both phases are related to uplift and denudation of an inherited
33 palaeorelief, and stratigraphically preserved as distinct angular discordances and
34 paraconformities involving gaps of up to 22 m.y. The geochemical features of the
35 Toledanian and Sardic, felsic-dominant activities point to a predominance of magmatic
36 byproducts derived from the melting of metasedimentary rocks, rich in SiO₂ and K₂O
37 and with peraluminous character. Zr/TiO₂, Zr/Nb, Nb/Y and Zr vs. Ga/Al ratios, and
38 REE and $\varepsilon\text{Nd}_{(\text{t})}$ values suggest the contemporaneity, for both phases, of two
39 geochemical scenarios characterized by arc and extensional features evolving to
40 distinct extensional and rifting conditions associated with the final outpouring of mafic
41 tholeiitic-dominant lava flows. The Toledanian and Sardic magmatic phases are linked
42 to neither metamorphism nor penetrative deformation; on the contrary, their
43 unconformities are associated with foliation-free open folds subsequently affected by
44 the Variscan deformation. The geochemical and structural framework precludes
45 subduction generated melts reaching the crust in a magmatic arc to back-arc setting,
46 but favours partial melting of sediments and/or granitoids in a continental lower crust
47 triggered by the underplating of hot mafic magmas related to the opening of the Rheic
48 Ocean.

49 **Keywords:** granite, orthogneiss, geochemistry, Cambrian, Ordovician, Gondwana.

50

51

52 **1. Introduction**

53

54 A succession of Early–Palaeozoic magmatic episodes, ranging in age from Furongian
55 (former “late Cambrian”) to Late Ordovician, is widespread along the south-western
56 European margin of Gondwana. Magmatic pulses are characterized by preferential
57 development in different palaeogeographic areas and linked to the development of
58 stratigraphic unconformities, but they are related to neither metamorphism nor
59 penetrative deformation (Gutiérrez Marco et al., 2002; Montero et al., 2007). In the
60 Central Iberian Zone of the Iberian Massif (representing the western branch of the
61 Ibero-Armorican Arc; Fig. 1A–B), this magmatism is mainly represented by the Ollo de
62 Sapo Formation, which has long been recognized as a Furongian–Early Ordovician
63 (495–470 Ma) assemblage of felsic-dominant volcanic, subvolcanic and plutonic
64 igneous rocks. This magmatic activity is contemporaneous with the development of the
65 Toledanian Phase, which places Lower Ordovician (upper Tremadocian–Floian) rocks
66 onlapping an inherited palaeorelief formed by Ediacaran–Cambrian rocks and involving
67 a sedimentary gap of ca. 22 m.y. This unconformity can be correlated with the
68 “Furongian gap” identified in the Ossa-Morena Zone of the Iberian Massif and the Anti-
69 Atlas Ranges of Morocco (Álvaro et al., 2007, 2018; Álvaro and Vizcaíno, 2018;
70 Sánchez-García et al., 2019), and with the “lacaune normande” in the central and
71 North-Armorican Domains (Le Corre et al., 1991).

72 Another felsic-dominant magmatic event, although younger (Early–Late Ordovician)
73 in age, has been recognized in some massifs situated along the eastern branch of the
74 Variscan Ibero-Armorican Arc, such as the Pyrenees, the Occitan Domain and Sardinia
75 (Fig. 1A, C–E). This magmatism is related to the Sardic unconformity, where
76 Furongian–Lower Ordovician rocks are unconformably overlain by those attributed to
77 the Sandbian–lower Katian (former Caradoc). The Sardic Phase is related to a
78 sedimentary gap of ca. 16–20 m.y. and geometrically ranges from 90° (angular

79 discordance) to 0° (paraconformity) (Barca and Cherchi, 2004; Funneda and Oggiano,
80 2009; Álvaro et al., 2016, 2018; Casas et al., 2019).

81 Although a general consensus exists to associate this Furongian–Ordovician
82 magmatism with the opening of the Rheic Ocean and the drift of Avalonia from
83 northwestern Gondwana (Díez Montes et al., 2010; Nance et al., 2010; Thomson et al.,
84 2010; Álvaro et al., 2014a), the origin of this magmatism has received different
85 interpretations. In the Central Iberian Zone, for instance, **several geodynamic models**
86 **have been proposed, such as:** (i) **subduction-related melts** reaching the crust in a
87 magmatic arc to back-arc setting (Valverde-Vaquero and Dunning, 2000; Castro et al.,
88 2009); (ii) partial melting of sediments or granitoids in a continental lower crust affected
89 by the underplating of hot mafic magmas during an extensional regime (Bea et al.,
90 2007; Montero et al., 2009; Díez Montes et al., 2010); and (iii) post-collisional
91 decompression melting of an earlier thickened continental crust, and without significant
92 mantle involvement (Villaseca et al., 2016). In the Occitan Domain (southern French
93 Massif Central and Mouthoumet massifs) and the Pyrenees, Marini (1988), Pouclet et
94 al. (2017) and Puddu et al. (2019) have suggested a link to mantle thermal anomalies.
95 Navidad et al. (2018) proposed that the Pyrenean magmatism was induced by
96 progressive crustal thinning and uplift of lithospheric mantle isol terms. In Sardinia,
97 Oggiano et al. (2010), Carmignani et al. (2001), Gaggero et al. (2012) and Cruciani et
98 al. (2018) have suggested that a subduction scenario, mirroring an Andean-type active
99 margin, **caused** the main Mid–Ordovician magmatic activity. In the Alps, the Sardic
100 counterpart is also interpreted as a result of the collision of the so-called Qaidam Arc
101 with the Gondwanan margin, subsequently followed by the accretion of the Qilian Block
102 (Von Raumer and Stampfli, 2008; Von Raumer et al., 2013, 2015). This geodynamic
103 interpretation is mainly suggested for the Alpine Briançonnais-Austroalpine basement,
104 where the volcanosedimentary complexes postdating the Sardic tectonic inversion and
105 folding stage portray a younger arc-arc oblique collision (450 Ma) of the eastern tail of
106 the internal Alpine margin with the Hun terrane, succeeded by conspicuous exhumation

107 in a transform margin setting (430 Ma) (Zurbriggen et al., 1997; Schaltegger et al.,
108 2003; Franz and Romer, 2007; Von Raumer and Stampfli, 2008; Von Raumer et al.,
109 2013; Zurbriggen, 2015, 2017).

110 Until now the Toledanian and Sardic magmatic events had been studied on different
111 areas and interpreted separately, without taking into account their similarities and
112 differences. In this work, the geochemical affinities of the Furongian–Early Ordovician
113 (Toledanian) and Early–Late Ordovician (Sardic) felsic magmatic activities recorded in
114 the Central Iberian and Galicia-Trás-os-Montes Zones, Pyrenees, Occitan Domain and
115 Sardinia are compared. The re-appraisal is based on 17 new samples from the
116 Pyrenees, Montagne Noire and Sardinia, completing the absence of analysis in these
117 areas and wide-ranging a dataset of 93 previously published geochemical analyses
118 throughout the study region in south-western Europe. This comparison may contribute
119 to a better understanding of the meaning and origin of this felsic magmatism, and thus,
120 to discuss the geodynamic scenario of this Gondwana margin (Fig. 1A) during
121 Cambrian–Ordovician times, bracketed between the Cadomian and Variscan
122 orogenies.

123

124 2. Emplacement and age of magmatic events

125

126 This section documents the emplacement (summarized in Fig. 2) and age (Fig. 3) of
127 the Toledanian and Sardic magmatic events throughout a SW-NE palaeogeographic
128 transect of the south-western European margin of Gondwana during Cambro–
129 Ordovician times.

130

131 2.1. Iberian Massif

132

133 In the Ossa Morena and southern Central Iberian Zones of the Iberian Massif (Fig. 1A–
134 B), the so-called Toledanian Phase is recognized as an angular discordance that

135 separates variably tilted Ediacaran–Cambrian Series 2 rifting volcanosedimentary
136 packages from overlying passive-margin successions. The Toledanian gap comprises,
137 at least, most of the Furongian and basal Ordovician, but the involved erosion can
138 incise into the entire Cambrian and the upper Ediacaran Cadomian basement
139 (Gutiérrez-Marco et al., 2019; Álvaro et al., 2019; Sánchez-García et al., 2019).
140 Recently, Sánchez-García et al. (2019) have interpreted the Toledanian Phase as a
141 break-up (or rift/drift) unconformity with the Armorican Quartzite (including the Purple
142 Series and Los Montes Beds; McDougall et al., 1987; Gutiérrez-Alonso et al., 2007;
143 Shaw et al., 2012, 2014) sealing an inherited Toledanian palaeorelief ([Fig. 2](#)).

144 The phase of uplift and denudation of an inherited palaeorelief composed of upper
145 Ediacaran–Cambrian rocks is associated with the massive outpouring of felsic-
146 dominant calc-alkaline magmatic episodes related to neither metamorphic nor cleavage
147 features. This magmatic activity is widely distributed throughout several areas of the
148 Iberian Massif, such as the Cantabrian Zone and the easternmost flank of the West
149 Asturian-Leonese Zone, where sills and rhyolitic lava flows and volcaniclastics mark
150 the base of the Armorican Quartzite (dated at **ca.** 477.5 Ma; Gutiérrez-Alonso et al.,
151 2007, 2016), and the lower Tremadocian Borrachón Formation of the Iberian Chains
152 (Álvaro et al., 2008). Similar ages have been reported **from** igneous rocks of the Basal
153 Allochthonous Units and the Schistose Domain in the Galicia-Trás-os-Montes Zone
154 (500–462 Ma; Valverde-Vaquero et al., 2005, 2007; Montero et al., 2009; Talavera et
155 al., 2008, 2013; Dias da Silva et al., 2012, 2014; Díez Fernández et al., 2012; Farias et
156 al., 2014) and different areas of the Central Iberian Zone, including the contact
157 between the Central Iberian and Ossa-Morena Zones, where the Carrascal and
158 Portalegre batoliths are intruded and the felsic volcanosedimentary Urra Formation
159 **marks the unconformity that separates Cambrian and Ordovician strata** (494–470 Ma,
160 Solá et al., 2008; Antunes et al., 2009; Neiva et al., 2009; Romaõ et al., 2010; Rubio-
161 Ordóñez et al., 2012; Villaseca et al., 2013) ([Fig. 1B](#)).

162 The most voluminous Toledanian-related volcanic episode is represented by the
163 Ollo de Sapo Formation, which **crops out throughout** the northeastern Central Iberian
164 Zone. It mainly consists of felsic volcanosedimentary and volcanic rocks, interbedded
165 at the base of the Lower Ordovician strata and plutonic bodies. The Ollo de Sapo
166 volcanosedimentary Formation has long been recognized as an enigmatic Furongian–
167 Early Ordovician (495–470 Ma) magmatic event exposed along the core of a 600 km-
168 long antiform (labelled as 77 in Fig. 1B) (Valverde-Vaquero and Dunning, 2000; Bea et
169 al., 2006; Montero et al., 2007, 2009; Zeck et al., 2007; Castiñeiras et al., 2008a; Díez
170 Montes et al., 2010; Navidad and Castiñeiras, 2011; Talavera et al., 2013; López-
171 Sánchez et al., 2015; Díaz-Alvarado el al., 2016; Villaseca et al., 2016; García-Arias et
172 al., 2018). The peak of magmatic activity was reached at ca. 490–485 Ma and its most
173 recognizable characteristic is the presence of abundant megacrysts of K-feldspar,
174 plagioclase and blue quartz. There is no evident space-time relationship in its
175 distribution (for a discussion, see López-Sánchez et al., 2015) and, collectively, the
176 Ollo de Sapo Formation rocks **record** a major tectonothermal event whose expression
177 can be found in most of the Variscan massifs of continental Europe including the
178 Armorican and Bohemian massifs (e.g., von Quadt, 1997; Kröner and Willmer, 1998;
179 Linnemann et al., 2000; Tichomirowa et al., 2001; Friedl et al., 2004; Mingram et al.,
180 2004; Teipel et al., 2004; Ballèvre et al., 2012; El Korh et al., 2012; Tichomirowa et al.,
181 2012; for a summary, see Casas and Murphy, 2018). The large **volume** of magmatic
182 rocks located in the European Variscan Belt led some authors to propose the existence
183 of a siliceous Large Igneous Province (LIP) (Díez Montes et al., 2010; Gutiérrez-Alonso
184 et al., 2016), named Ibero-Armorican LIP by García-Arias et al. (2018).

185

186 **2.2. Central and Eastern Pyrenees**

187

188 In the **central and eastern** Pyrenees (Fig. 1D), earliest Ordovician volcanic-free
189 passive-margin conditions, represented by the Jujols Group (Padel et al., 2018), were

190 succeeded by a late Early–Mid Ordovician phase of uplift and erosion that led to the
191 onset of the Sardic unconformity (Fig. 2). Uplift was associated with magmatic activity,
192 which continued until Late Ordovician times. An extensional interval took place then
193 developing normal faults that controlled the sedimentation of post–Sardic siliciclastic
194 deposits infilling palaeorelief depressions. Acritarchs recovered in the uppermost part
195 of the Jujols Group suggest a broad Furongian–earliest Ordovician age (Casas and
196 Palacios, 2012), conterminous with a maximum depositional age of ca. 475 Ma, based
197 on the age of the youngest detrital zircon populations (Margalef et al., 2016). On the
198 other hand, a ca. 459 Ma U–Pb age for the Upper Ordovician volcanic rocks overlying
199 the Sardic Unconformity has been proposed in the eastern Pyrenees (Martí et al.,
200 2019), and ca. 452–455 Ma in the neighbouring Catalan Coastal Ranges, which
201 represent the southern prolongation of the Pyrenees (Navidad et al., 2010; Martínez et
202 al., 2011). Thus, a time gap of about 16–23 m.y. can be related to the Sardic Phase in
203 the eastern Pyrenees and the neighbouring Catalan Coastal Ranges.

204 Coeval with the late Early–Mid Ordovician phase of generalized uplift and
205 denudation, a key magmatic activity led to the intrusion of voluminous granitoids, about
206 500 to 3000 m thick and encased in strata of the Ediacaran–Lower Cambrian
207 Canaveilles Group (Fig. 2). These granitoids constitute the protoliths of the large
208 orthogneissic laccoliths that punctuate the backbone of the central and eastern
209 Pyrenees. These are, from west to east (Fig. 1D), the Aston (467–470 Ma ; Denèle et
210 al., 2009; Mezger and Gerdes, 2016), Hospitalet (about 472 Ma, Denèle et al., 2009),
211 Canigó (472–462 Ma, Cocherie et al., 2005; Navidad et al., 2018), Roc de Frausa
212 (477–476 Ma; Cocherie et al., 2005; Castiñeiras et al., 2008b) and Albera (about 470
213 Ma; Liesa et al., 2011) massifs, which comprise a dominant Floian–Dapingian age. It is
214 noticeable the fact that only a minor representation of coeval basic magmatic rocks are
215 outcropped. The acidic volcanic equivalents have been documented in the Albera
216 massif, where subvolcanic rhyolitic porphyroid rocks have yielded similar ages to those

217 of the main gneissic bodies at **about** 474–465 Ma (Liesa et al., 2011). Similar acidic
218 byproducts are represented by the rhyolitic sills of Pierrefite (Calvet et al., 1988).

219 The late Early–Mid Ordovician (“Sardic”) phase of uplift was succeeded by a Late
220 Ordovician extensional **interval** responsible for the opening of (half-)grabens infilled
221 with the basal Upper Ordovician alluvial-to-fluvial conglomerates (La Rabassa
222 **Conglomerate Formation**). At **map** scale, a set of NE-SW trending normal faults
223 abruptly **controlling** the thickness of the basal Upper Ordovician formations can be
224 recognized in the La Cerdanya area (Casas and Fernández, 2007; Casas, 2010).
225 Sharp variations in the thickness of the Upper Ordovician strata have been
226 documented by Harteveld (1970) and Casas and Fernández (2007). Drastic variations
227 in grain size and thickness can be attributed to the development of palaeotopographies
228 controlled by faults and subsequent erosion of uplifted palaeoreliefs, with subsequent
229 infill of depressed areas by alluvial fan and fluvial deposits, finally sealed by Silurian
230 sediments (Puddu et al., 2019). A Late Ordovician magmatic pulse**e** contemporaneously
231 yielded a varied set of magmatic rocks. Small granitic bodies are encased in the
232 Canaveilles strata of the Canigó massif. They constitute the protoliths of the Cadí
233 (**about** 456 Ma; Casas et al., 2010), Casemí (446 **to** 452 Ma; Casas et al., 2010), Núria
234 (**ca.** 457 Ma; Martínez et al., 2011) and Canigó G-1 type (**ca.** 457 Ma; Navidad et al.,
235 2018) gneisses.

236 The lowermost part of the Canaveilles Group (the so-called Balaig Series) host
237 metre-scale thick bodies of metadiorite **sills** related to an Upper Ordovician protolith,
238 (**ca.** 453 Ma, SHRIMP U–Pb in zircon; Casas et al., 2010). Coeval calc-alkaline
239 ignimbrites, andesites and volcaniclastic rocks are interbedded in the Upper Ordovician
240 succession of the Bruguera and Ribes de Freser areas (Robert and Thiebaut, 1976;
241 Ayora, 1980; Robert, 1980; Martí et al., 1986, 2019). In the Ribes area, a granitic body
242 with granophyric texture, dated at **ca.** 458 Ma by Martínez et al. (2011), intruded at the
243 base of the Upper Ordovician succession. In the La Pallaresa dome, some metre-scale
244 rhyodacitic to dacitic subvolcanic sills, Late Ordovician in age (ca. 453 Ma, Clariana et

245 al., 2018), occur interbedded within the pre-unconformity strata and close to the base
246 of the Upper Ordovician.

247

248 **2.3. Occitan Domain: Albigeois, Montagne Noire and Mouthoumet massifs**

249

250 The parautochthonous framework of the southern French Massif Central, named
251 Occitan Domain by Pouclet et al. (2017), includes among others, from south to north,
252 the Mouthoumet, Montagne Noire and Albigeois massifs. The domain represents the
253 southeastern prolongation of the Variscan South Armorican Zone (including
254 southwestern Bretagne and Vendée). Since Gèze (1949) and Arthaud (1970), the
255 southern edge of the French Massif Central has been traditionally subdivided, from
256 north to south, into the northern, axial and southern Montagne Noire ([Fig. 1C](#)). The
257 Palaeozoic succession of the northern and southern sides includes sediments ranging
258 from late Ediacaran to Silurian and from Terreneuvian (Cambrian) to Visean in age,
259 respectively. These successions are affected by large scale, south-verging recumbent
260 folds that display a low to moderate metamorphic grade. Their emplacement took place
261 in Late Visean to Namurian times (Engel et al., 1980; Feist and Galtier, 1985; Echtler
262 and Malavieille, 1990). The Axial Zone consists of plutonic, migmatitic and
263 metamorphic rocks **forming a regional ENE-WSW oriented dome** ([Fig. 1C](#)), where four
264 principal lithological units can be recognized (i) schists and micaschists, (ii) migmatitic
265 orthogneisses, (iii) metapelitic metatexites, and (iv) diatexites and granites (Cocherie,
266 2003; Faure et al., 2004; Roger et al., 2004, 2015; Bé Mézème, 2005; Charles et al.,
267 2009; Rabin et al., 2015). The Rosis micaschist synform subdivides the eastern Axial
268 Zone into the Espinouse and Caroux sub-domes, whereas the southwestern edge of
269 the Axial Zone comprises the Nore massif.

270 In the Occitan Domain, two main Cambro–Ordovician felsic events can be identified
271 giving rise to the protoliths of (i) the Larroque metarhyolites in the northern Montagne

272 Noire and Albigeois, thrusted **southward** from Rouergue; and (ii) the migmatitic
273 ortogneisses **that form** the Axial Zone of the Montagne Noire ([Fig. 2](#)).

274 (i) The Larroque volcanosedimentary Complex is a thick (500–1000 m) package of
275 porphyroclastic metarhyolites located on the northern Montagne Noire (Lacaune
276 Mountains), Albigeois (St-Salvi-de-Carcavès and St-Sernin-sur-Rance nappes) and
277 Rouergue; the Variscan setting of the formation is allochthonous in the Albigeois and
278 parautochthonous in the rest. **This volcanism emplaced above the Furongian strata and**
279 **the so-called “Série schisto-gréseuse verte”** (see Guérangé-Lozes et al., 1996;
280 Guérangé-Lozes and Alabouvette, 1999), and is encased in the upper part of the
281 **Miaolingian La Gardie Formation** (Pouclet et al., 2017) ([Fig. 2](#)). The Larroque volcanic
282 rocks consist of deformed porphyroclastic rhyolites rich in largely fragmented, lacunous
283 (rhyolitic) quartz and alkali feldspar phenocrysts. The metarhyolites occur as porphyritic
284 lava flows, sills and other associated facies, such as aphyric lava flows, porphyritic and
285 aphyric pyroclastic flows of welded or unwelded ignimbritic types, fine to coarse tephra
286 deposits, and epiclastic and volcaniclastic deposits. **These rocks are named “augen**
287 **gneiss” or **augengneiss** and** do not display a high-grade gneiss paragenesis but a
288 general lower grade metamorphic mineralogy. The Occitan augengneisses mimic the
289 Ollo de Sapo facies from the Central Iberian Zone because of their large bluish quartz
290 phenocrysts. Based on geochemical similarities and contemporaneous emplacement,
291 Pouclet et al. (2017) suggested that this event also supplied the Davejean acidic
292 volcanic rocks in the Mouthoumet Massif, which represent the southern prolongation of
293 the Montagne Noire ([Fig. 2](#)), and the Génis rhyolitic unit of the western Limousin
294 sector.

295 (ii) Some migmatitic orthogneisses make up the southern Axial Zone, from the
296 western Cabardès to the eastern Caroux domes. The orthogneisses, derived from
297 Ordovician metagranites bearing large K-feldspar phenocrysts, were emplaced at
298 **about** 471 Ma (Somail Orthogneiss, Cocherie et al., 2005), 456 **to** 450 Ma (Pont de
299 Larn and Gorges d'Héric gneisses, Roger et al., 2004) and **ca.** 455 Ma (Sain Eutrope

300 gneiss, Pitra et al., 2012). They intruded a metasedimentary pile, traditionally known as
301 “Schistes X” and formally named St. Pons-Cabardès Group ([Fig. 2](#)). The latter consists
302 of schists, greywackes, quartzites and subsidiary volcanic tuffs and marbles (Demange
303 et al., 1996; Demange, 1999; Alabouvette et al., 2003; Roger et al., 2004; Cocherie et
304 al., 2005). The group is topped by the Sériès Tuff, dated at [about](#) 545 Ma (Lescuyer
305 and Cocherie, 1992), which represents a contemporaneous equivalent of the
306 Cadomian Riverous rhyolitic tuff (542.5 [to](#) 537.1 Ma) from the Lodève inlier of the
307 northern Montagne Noire (Álvaro et al., 2014b, 2018; Padel et al., 2017). [Age of](#)
308 [migmatization has been inferred from U–Pb dates on](#) monacite from migmatites and
309 anatetic granites at 333 [to](#) 327 Ma (Bé Mézème, 2005; Charles et al., 2008); as a
310 result, the 330–325 Ma time interval can represent a Variscan crustal melting event in
311 the Axial Zone.

312 As in the Pyrenees, the Middle Ordovician is absent in the Occitan Domain. Its gap
313 allows distinction between a Lower Ordovician pre-unconformity sedimentary package
314 para- to unconformably overlain by an Upper Ordovician–Silurian succession (Álvaro et
315 al., 2016; Pouclet et al., 2017).

316

317 **2.4. Sardinia**

318

319 In Sardinia the Cambro–Ordovician magmatism is well represented in the external
320 (southern) and internal (northern) nappe zones of the exposed Variscan Belt ([Fig. 1E](#)),
321 and ranges in age from late Furongian to Late Ordovician. A Furongian–Tremadocian
322 (ca. 491–480 Ma) magmatic activity, predating the Sardic phase, is mostly represented
323 by felsic volcanic and subvolcanic rocks encased in the San Vito sandstone Formation.
324 The Sardic-related volcanic products differ from one nappe to another: intermediate
325 and basic (mostly metandesites and andesitic basalts) are common in the nappe
326 stacking of the central part of the island (Barbagia and Goceano), whereas felsic
327 metavolcanites prevail in the southeastern units. Their age is bracketed between 465

328 and 455 Ma (Giacomini et al., 2006; Oggiano et al., 2010; Pavanetto et al., 2012;
329 Cruciani et al., 2018) and matches the Sardic gap based on biostratigraphy (Barca et
330 al., 1988).

331 Teichmüller (1931) and Stille (1939) were the first to recognize in southwestern
332 Sardinia an intra-Ordovician stratigraphic hiatus. Its linked erosive unconformity is
333 supported by a correlatable strong angular discordance in the Palaeozoic basement of
334 the Iglesiente-Sulcis area, External Zone (Carmignani et al., 2001). This major
335 discontinuity separates the Cambrian–Lower Ordovician Nebida, Gonnese and Iglesias
336 groups (Pillola et al., 1998) from the overlying coarse-grained (“Puddinga”) Monte
337 Argentu metasediments (Leone et al., 1991, 2002; Laske et al., 1994). The gap
338 comprises a chronostratigraphically constrained minimum gap of about 18 m.y. that
339 includes the Floian and Dapingian (Barca et al., 1987, 1988; Pillola et al., 1998; Barca
340 and Cherchi, 2004) (Fig. 2). The hiatus is related to neither metamorphism nor
341 cleavage, though some E–W folds have been documented in the Gonnese Anticline
342 and the Iglesias Syncline (Cocco et al., 2018), which are overstepped by the
343 “Puddinga” metaconglomerates. Both the E–W folds and the overlying
344 metaconglomerates were subsequently affected by Variscan N–S folds (Cocco and
345 Funnedo, 2011, 2017). Sardic-related volcanic rocks are not involved in this area, but
346 Sardic-inherited palaeoreliefes are lined with breccia slides that include metre- to
347 decametre-scale carbonate boulders (“Olistoliti”), some of them hosting
348 synsedimentary faults contemporaneously mineralized with ore bodies (Boni and
349 Koeppel, 1985; Boni, 1986; Barca, 1991; Caron et al., 1997). The lower part of the
350 unconformably overlying Monte Argentu Formation deposited in alluvial to fluvial
351 environments (Martini et al., 1991; Loi et al., 1992; Loi and Dabard, 1997).

352 A similar gap was reported by Calvino (1972) in the Sarrabus-Gerrei units of the
353 External Nappe Zone. The so-called “Sarrabese Phase” is related to the onset of thick,
354 up to 500 m thick, volcanosedimentary complexes and volcanites (Barca et al., 1986;
355 Di Pisa et al., 1992) with a Darriwilian age for the protoliths of the metavolcanic rocks

356 (465.4 to 464 Ma; Giacomini et al., 2006; Oggiano et al., 2010). In the Iglesiente-Sulcis
357 region (Fig. 1E), Carmignani et al. (1986, 1992, 1994, 2001) suggested that the
358 “Sardic-Sarrabese phase” should be associated with the compression of a Cambro–
359 Ordovician back-arc basin that originated the migration of the Ordovician volcanic arc
360 toward the Gondwanan margin.

361 Some gneissic bodies, interpreted as the plutonic counterpart of metavolcanic rocks,
362 are located in the Bithia unit (e.g., the Monte Filau area, 458 to 457 Ma, surrounded by
363 a Mid-Ordovician andalusite thermal aureole; Pavanello et al., 2012; Costamagna et
364 al., 2016) and in the internal units (Lodè orthogneiss, ca. 456 Ma; Tanaunella
365 orthogneiss, ca. 458 Ma, Helbing and Tiepolo, 2005; Golfo Aranci orthogneiss, ca. 469
366 Ma, Giacomini et al., 2006).

367 The Sardic palaeorelief is sealed by Upper Ordovician transgressive deposits. The
368 sedimentary facies show high variability, but the –mostly terrigenous– sediments vary
369 from grey fine- to medium-sized sandstones, to muddy sandstones and mudstones.
370 They are referred to the Katian Punta Serpeddì and Orroeledu formations (Pistis et al.,
371 2016). This post-Sardic sedimentary succession is coeval with a new magmatic
372 pulsation represented by alkaline to tholeiitic within-plate basalts (Di Pisa et al., 1992;
373 Gaggero et al., 2012).

374

375 **3. Geochemical data**

376

377 **3.1. Materials and methods**

378

379 The rocks selected for geochemical analysis (231 samples; see tectonostratigraphic
380 location in Fig. 1 and stratigraphic emplacement in Fig. 2) have recorded different
381 degrees of hydrothermalism and metamorphism, as a result of which only the most
382 immobile elements have been considered. The geochemical calculations, in which the

383 major elements take part, have been made from values recalculated to 100 in volatile
384 free compositions; Fe is reported as FeO_t.

385 The geochemical dataset of the Central Iberian Zone includes 152 published
386 geochemical data, from which 85 are plutonic and 67 volcanic and volcanioclastic rocks
387 from the Ollo de Sapo Formation (Galicia, Sanabria and Guadarrama areas), and the
388 contact between the Central Iberian and Ossa Morena Zones (Urra Formation and
389 Portalegre and Carrascal granites). Other data were yielded from six volcanic rocks of
390 the Galicia-Trás-os-Montes Zone (Saldanha area) ([Fig. 1B; Repository Data](#)).

391 The dataset of the eastern Pyrenees consists of 38 samples, six of which are upper
392 Lower Ordovician volcanic rocks, and seven upper Lower Ordovician plutonic rocks,
393 together with nine Upper Ordovician volcanic and 14 Upper Ordovician plutonic rocks
394 ([Repository Data](#)). New data reported below include two samples of subvolcanic sills
395 intercalated in the pre-Sardic unconformity succession (Clariana et al., 2018; Margalef,
396 unpubl.; [Table 1](#)).

397 The study samples from the Occitan Domain comprise six metavolcanic rocks, four
398 from the Larroque volcanosedimentary Complex in the Albigeois and northern
399 Montagne Noire and two from the Mouthoumet massif (Pouclet et al., 2017)
400 ([Repository Data](#)), and four new samples for the Axial Zone gneisses ([Table 1](#)).

401 In the Sardinian dataset, 25 published analyses are selected: five correspond to the
402 Golfo Aranci orthogneiss (Giacomini et al., 2006), six to metavolcanics from the central
403 part of the island (Giacomini et al., 2006; Cruciani et al., 2013), and five to
404 metavolcanics and one to gneisses from the Bithia unit (Cruciani et al., 2018)
405 ([Repository Data](#)). Ten new analyses are added from the Monte Filau and Capo
406 Spartivento gneisses of the Bithia unit, and from the Punta Bianca gneisses embedded
407 within the migmatites of the High-grade Metamorphic complex of the Inner Zone ([Table](#)
408 [1](#)).

409 Whole-rock major and trace elements and rare earth element (REE) compositions
410 were determined at ACME Laboratories, Vancouver, Canada. LiBO₂ fusion followed by

411 X-ray fluorescence spectroscopy (XRF) analysis was used to determine major
412 elements. Rare earth and refractory elements were measured by ICP–MS following a
413 lithium metaborate/tetraborate fusion and nitric acid digestion on 0.2 g of sample. For
414 base metals, 0.5 g of sample was digested in Aqua Regia at 95 °C and analyzed by
415 inductively coupled plasma - atomic emission spectrometry (ICP–AES). Analyses of
416 standards and duplicate samples indicate precision to better than 1 % for major oxides,
417 and 3–10 % for minor and trace elements.

418 Additional Sm–Nd isotopic analyses were performed at Centro de Geocronología y
419 Geoquímica Isotópica from the Complutense University, Madrid. They were carried out
420 in whole-rock powders using a ^{150}Nd – ^{149}Sm tracer by isotope dilution-thermal ionization
421 mass spectrometry (ID-TIMS). The samples were first dissolved through oven
422 digestion in sealed Teflon bombs with ultra pure reagents to perform two-stage
423 conventional cation-exchange chromatography for separation of Sm and Nd (Strelow,
424 1960; Winchester, 1963), and subsequently analysed using a Sector 54 VG-Micromass
425 multicollector spectrometer. The measured $^{143}\text{Nd}/^{144}\text{Nd}$ isotopic ratios were corrected
426 for possible isobaric interferences from ^{142}Ce and ^{144}Sm (only for samples with
427 $^{147}\text{Sm}/^{144}\text{Sm} < 0.0001$) and normalized to $^{146}\text{Nd}/^{144}\text{Nd} = 0.7219$ to correct for mass
428 fractionation. The Lajolla Nd international isotopic standard was analysed during
429 sample measurement, and gave an average value of $^{143}\text{Nd}/^{144}\text{Nd} = 0.5114840$ for 9
430 replicas, with an internal precision of ± 0.000032 (2σ). These values were used to
431 correct the measured ratios for possible sample drift. The estimated error for the
432 $^{147}\text{Sm}/^{144}\text{Nd}$ ratio is 0.1%.

433 A general classification of the analyzed samples, following Winchester and Floyd
434 (1977), can be seen in Figure 4A–B, and the geographical coordinates of the new
435 samples in Table 1. For geochemical comparison (summarized in Table 2), two large
436 groups or suites are differentiated in order to check the similarities and differences
437 between the magmatic rocks, and to infer a possible geochemical trend following a

438 palaeogeographic SW–NE transect. The description reported below follows the same
439 palaeogeographic and chronological order.

440

441 **3.2. Furongian–to–Mid Ordovician Suite**

442

443 In the Central Iberian and Galicia-Trás-os-Montes Zones, the Furongian–to–Mid
444 Ordovician magmatic activity is pervasive. Their main representative is the Ollo de
445 Sapo Formation, which includes volcanic and subvolcanic rocks (67 samples) as well
446 as plutonic rocks (85 samples) (data from Murphy et al., 2006; Díez-Montes, 2007;
447 Montero et al., 2007, 2009; Solá, 2007; Solá et al., 2008; Talavera, 2009; Villaseca et
448 al., 2016). From the Parautochthon Schistose Domain of the Galicia-Trás-os Montes
449 Zone, six samples of rhyolite tuffs of the Saldanha Formation (Dias da Silva et al.,
450 2014) are selected, which share geochemical features with the Ollo de Sapo
451 Formation. **In summary, five facies are differentiated in the Central Iberian and Galicia-**
452 **Trás-os Montes Zones: the Ollo de Sapo orthogneisses, some leucogneisses,**
453 **metagranites and volcanic rocks, and the San Sebastián orthogneiss (for a**
454 **geochemical characterization, see Table 2).**

455 In the central and eastern Pyrenees, an Early–Mid Ordovician magmatic activity
456 gave rise to the intrusion of voluminous (about 500–3000 m in size) aluminous granitic
457 bodies, encased into the Canaveilles beds (Álvaro et al., 2018; Casas et al., 2019).
458 They constitute the protoliths of the large orthogneissic laccoliths that form the core of
459 the domal massifs scattered throughout the backbone of the Pyrenees. Rocks of the
460 Canigó, Roc de Frausa and Albera massifs have been taken into account in this work,
461 in which volcanic rocks of the Pierrefite and Albera massifs, and the so-called G2 and
462 G3 orthogneisses by Guitard (1970) are also included. All subgroups vary
463 compositionally from subalkaline andesite to rhyolite, as illustrated in the Pearce's
464 (1996) diagram of [Figure 5](#) (data compiled from Vilà et al., 2005; Castiñeiras et al.,
465 2008b; Liesa et al., 2011; Navidad et al., 2018).

466 Although most rocks in this area are acidic, it is remarkable the presence of minor
467 mafic bodies (Cortalet and Marialles metabasites, not studied in this work), which could
468 indicate a mantle connection with parental magmas during the Mid and Late
469 Ordovician. As well, it should be noted that there are no andesitic rocks in the area.

470 In the Occitan Domain, six samples of the Larroque volcanosedimentary Complex
471 (Early Tremadocian in age) represent basin floors and subaerial explosive and effusive
472 rhyolites (Pouclet et al., 2017). The porphyroclastic rocks of the Larroque metarhyolites
473 were sampled in the Saint-Géraud and Larroque areas from the Saint-Sernin-sur-
474 Rance nappe and the Saint-André klippe above the Saint-Salvi-de-Carcavès nappe
475 (Pouclet et al., 2017).

476 In the Middle Ordovician rocks of Sardinia, 11 samples are selected, five of which
477 correspond to orthogneisses of the Aranci Gulf, in the Inner Zone of the NE island
478 (Giacomini et al., 2006), completed with six volcanic rocks of the External Zone
479 (Giacomini et al., 2006; Cruciani et al., 2018) ([Table 2](#)).

480

481 **3.3 Upper Ordovician Suite**

482

483 In the central and eastern Pyrenees, four Upper Ordovician subgroups are
484 distinguished based on their field occurrence and geochemical and geochronological
485 features: the G1-type orthogneisses *sensu* Guitard (1970); the Cadí and Casemí
486 orthogneisses and the metavolcanic rocks that include the Ribes de Freser rhyolites;
487 the Els Metges volcanic tuffs; and the rhyolites from Andorra and Pallaresa areas (the
488 latter dated at ca. 453 Ma; Clariana et al., 2018) ([Table 2](#)). The suite is completed with
489 the Somail orthogneisses of the Axial Montagne Noire (dated at ca. 450 Ma at Gorges
490 d'Héric; Roger et al., 2004) and the orthogneisses from the Sardinian External Zone
491 (dated at ca. 458–457 Ma at Monte Filau; Pavanetto et al., 2012) and the volcanic rocks
492 from the Sardinian Nappe Zone ([Table 2](#)).

493

494 **4. Geochemical framework**

495

496 A geochemical comparison between the Furongian–Ordovician felsic rocks of all the
497 above-reported groups offers the opportunity to characterize the successive sources of
498 crustal-derived melts along the south-western European margin of Gondwana.

499 The geochemical features point to a predominance of materials derived from the
500 melting of metasedimentary rocks, rich in SiO_2 and K_2O (average $\text{K}_2\text{O}/\text{Na}_2\text{O} = 2.25$)
501 and peraluminous ($0.4 < \text{C}_{\text{norm}} < 4.5$ and $0.94 < \text{A/CNK} > 3.12$), with only three samples
502 with $\text{A/CNK} < 1$ (samples 100786 of the Casemí subgroup, and T26 and T27 of the San
503 Sebastián subgroup).

504 The result of plotting the REE content vs. average values of continental crust
505 (Rudnick and Gao, 2004; [Fig. 6](#)) yields a flat spectra and a base level shared by most
506 of the considered groups. The total content in REE is moderate to high (average REE =
507 176 ppm, ranging between 482.2 and 26.0 ppm; [Fig. 7](#)), with a maximum in the
508 subgroup of the Middle Ordovician volcanic rocks from Sardinia (average REE = 335
509 ppm, VOL-SMO), and with LREE values more fractionated than HREE ones, and
510 negative anomalies of Eu, which would indicate a characteristic process of magmatic
511 evolution with plagioclase fractionation. These features are common in peraluminous
512 granitoids.

513 All subgroups display similar chondritic normalized REE patterns ([Fig. 7](#)), with an
514 enrichment in LREE relative to HREE, which should indicate the involvement of crustal
515 materials in their parental magmas. Nevertheless, some variations can be highlighted,
516 such as the lesser fractionation in REE content of some subgroups. These are the
517 leucogneisses from the Iberian massif (LG, $\text{La/Yb}_n = 2.01$), the Upper Ordovician
518 orthogneisses from Sardinia (OG-SUO, $\text{La/Yb}_n = 2.94$), the Casemí orthogneisses
519 ($\text{La/Yb}_n = 4.42$) and the Middle Ordovician volcanic rocks from Sardinia (OG-SUO,
520 $\text{La/Yb}_n = 2.94$). This may be interpreted as a greater degree of partial fusion in the
521 origin of their parental magmas (Rollinson, 1993).

522 There are three geochemical groups displaying $(\text{Gd}/\text{Yb})_n$ values > 2 , and $(\text{La}/\text{Yb})_n$
523 values ≥ 9 . These groups are OSS (Central Iberian Zone), VOL-OD (Occitan Domain)
524 and G1 (Pyrenees), and share higher alkalinity features.

525 Some V1 rocks from the Pyrenees (Pierrefite Formation) show no negative
526 anomalies in Eu. Their parental magmas could have been derived from deeper origins
527 and related to residual materials of the lower continental crust, in areas of production of
528 K-rich granites (Taylor and McLennan, 1989).

529 The spider diagrams ([Fig. 8](#)), however, exhibit strong negative anomalies in Nb, Sr
530 and Ti, which indicate a distinct crustal affiliation (Díez-Montes, 2007). Only the San
531 Sebastián orthogneisses (OSS) show distinct discrepancies in respect of the remaining
532 samples from the Ollo de Sapo Formation. They display lower negative anomalies in
533 Nb and a more alkaline character by comparison with the rest of the Ollo de Sapo
534 rocks, which point to alkaline affinities and greater negative anomalies in Nb.

535 Despite some small differences in the chemical ranges of some major elements,
536 most felsic Ordovician rocks from the Iberian massif (Central Iberian and Galicia-Trás-
537 os Montes Zones), eastern Pyrenees, Occitan Domain and Sardinia share a common
538 chemical pattern. The Lower–Middle Ordovician rocks of the eastern Pyrenees show
539 less variation in the content of Zr and Nb ([Fig. 8B](#)). The volcanic rocks of these groups
540 show a different REE behaviour, which would indicate different sources. Two groups
541 are distinguished in [Figure 7](#), one with greater enrichment in REE and negative
542 anomaly of Eu, and another with lesser content of HREE and without Eu negative
543 anomalies.

544 [Figure 9](#) illustrates how the average of all the considered groups approximates the
545 mean values of the Rudnick and Gao's (2003) upper continental crust (**UCC**). In this
546 figure, small deviations can be observed, some of them toward **lower continental crust**
547 (**LCC**) values and others toward **bulk continental crust** (**BCC**), indicating variations in
548 their parental magmas but with quite similar spectra. Overall chondrite-normalized

549 patterns are close to the values that represent the upper continental crust, with slight
550 enrichments in the Th/Nb, Th/La and Th/Yb ratios.

551 Finally, in the Occitan volcanic rocks (*VOL-OD*) the rare earth elements are enriched
552 and fractionated ($33.2 \text{ ppm} < \text{La} < 45.6 \text{ ppm}$; $11.2 < \text{La/Yb} < 14.5$). The upper
553 continental crust normalized diagram exhibits negative anomalies of Ti, V, Cr, Mn and
554 Fe associated with oxide fractionation, of Zr and Hf linked to zircon fractionation, and of
555 Eu related to plagioclase fractionation. The profiles are comparable to the Vendean
556 Saint-Gilles rhyolitic ones. The Th vs. Rb/Ba features are also similar to those of the
557 Saint-Gilles rhyolites, and the Iberian Ollo de Sapo and Urra rhyolites (Solá et al.,
558 2008; Díez Montes et al., 2010).

559

560 **4. Discussion**

561

562 **4.1 Inferred tectonic settings**

563

564 In order to clarify the evolution of geotectonic environments, the data have been
565 represented in different **discrimination** diagrams. The Zr/TiO₂ ratio (Lentz, 1996; Syme,
566 1998) is a key index of compositional evolution for intermediate and felsic rocks. In the
567 Syme diagram ([Fig. 10](#)), most rocks from the Central Iberian Zone represent a
568 characteristic arc association, although there are some contemporaneous samples
569 characterized by extensional-related values ($\text{Zr/Ti} = 0.10$, *LG*). The rocks of the
570 Middle–Ordovician San Sebastián orthogneisses (OSS) show values of $\text{Zr/Ti} = 0.08$,
571 intermediate between extensional and arc conditions. This could be interpreted as a
572 sharp change in geotectonic conditions toward the Mid Ordovician ([Fig. 10A](#)). For a
573 better comparison, the samples of the San Sebastián orthogneisses (OSS) and the
574 granites (GRA) have been distinguished with a shaded area in all the diagrams, since
575 they have slightly different characteristics to the rest of the samples from the Ollo de
576 Sapo group. The samples *G1* (Pyrenees) and *VOL* (Central Iberian Zone) broadly

577 share similar values, as a result of which, the three latter groups (OSS, G1 and VOL)
578 arrange following a good correlation line. The same trend seems to be inferred in the
579 eastern Pyrenees ([Fig. 10B](#)), where the Middle Ordovician subgroups display arc
580 features, but half of the Upper Ordovician subgroups show extensional affinities (G1
581 and Casemí orthogneisses). In the case of the Occitan orthogneisses ([Fig. 10C](#)), they
582 show arc characters, which contrast with the contemporaneous volcanic rocks
583 displaying extensional values with $Zr/Ti = 0.10$. This disparity between plutonic and
584 volcanic rocks could be interpreted as different conditions for the origin of these
585 magmas. In Sardinia ([Fig. 10D](#)), the same evolution from arc to extensional conditions
586 is highlighted for the Upper Ordovician samples, although some Middle Ordovician
587 volcanic rocks already shared extensional patterns ($Zr/Ti = 0.09$). In summary, there
588 seems to be a geochemical evolution in the Ordovician magmas grading from arc to
589 extensional environments.

590 In the Nb–Y tectonic discriminating diagram of Pearce et al. (1984) ([Fig. 11](#)), most
591 samples plot in the volcanic arc-type, though some subgroups project in the whitin-
592 plate and anomalous ORG. The majority of samples display very similar Zr/Nb and
593 Nb/Y ratios, typical of island arc or active continental margin rhyolites (Díez-Montes et
594 al., 2010). Only some samples plot separately: OSS samples with highest Nb contents
595 (>20 ppm), and some volcanic rocks of the Occitan Domain (average Nb =16.87 ppm).
596 In the eastern Pyrenees, the Middle Ordovician rocks plot in the volcanic arc field,
597 whereas the Upper Ordovician ones point in the ORG type, except the Casemí
598 samples. This progress of magmatic sources agrees with the evolution seen in [Figure](#)
599 [10](#). In the Ocitan Domain, VOL-OD samples share values with those of the San
600 Sebastián orthogneiss, while OG-OD shares values with those of OG from the Central
601 Iberian Zone.

602 The Zr vs. Nb diagram (Leat et al., 1986; modified by Piercy, 2011) ([Fig. 12](#))
603 illustrates how magmas evolved toward richer values in Zr and Nb, which is consistent
604 with what it is observed in the Syme diagram ([Fig. 10](#)). [Figure 12A](#) documents how

605 most samples show a general positive correlation. These different groups correspond
606 to the OSS and Portalegre granites, highlighted in the figure. The two groups indicate a
607 tendency toward alkaline magmas. Some samples, such as the Pyrenean G1, some
608 Occitan VOL-OD samples and some Sardinian OG-UOS samples share the same
609 affinity, clearly distinguished from the general geochemical trend exhibited by the
610 Central Iberian Zone.

611 On a Zr vs. Ga/Al diagram (Whalen et al., 1987) (Fig. 13), the samples depict an
612 intermediate character between anorogenic or alkaline (A-type) and orogenic (I&S-
613 type). In the Central Iberian Zone, samples from the San Sebastián orthogneisses and
614 Portalegre granites show characters of A-type granites, while the remaining samples
615 display affinities of I&S-type granites. For the Central Iberian Zone, a clear magmatic
616 shift toward more extensional geotectonic environments is characterized. For the
617 eastern Pyrenees, we find the same situation as in the Central Iberian Zone, with a
618 magmatic evolution toward A-granite type characteristics, indicating more extensional
619 geotectonic environments. In the Occitan Domain, the samples show a clear I&S
620 character. In the Sardinian case, the same seems to happen as in the Central Iberian
621 Zone: the Upper Ordovician orthogneisses suggest a more extensional character.

622 In summary, all the reported diagrams point to a magmatic evolution through time,
623 grading from arc to extensional geotectonic environments (with increased Zr/Ti ratios)
624 and to granite type-A characters. This geotectonic framework is consistent with that
625 illustrated in Figure 10. The geochemical characters of these rocks show a rhyodacite
626 to dacite composition, peraluminous and calc-alkaline K-rich character, and an arc-
627 volcanic affinity for most of samples, but without intermediate rocks associated with
628 andesitic types. Hence a change in time is documented toward more alkaline magmas.
629

630 **4.2 Interpretation of ε Nd values**

631

632 $\varepsilon\text{Nd}_{(\text{t})}$ values are useful to interpret the nature of magmatic sources. Most samples of
 633 the above-reported groups show no **significant** differences in isotopic $\varepsilon\text{Nd}_{(\text{t})}$ values, and
 634 Nd_{CHUR} model ages (Fig. 14). Some exceptions are related to granites from the
 635 southern Central Iberian Zone, which display positive values (from +2.6 to –2.4) and
 636 T_{DM} values from 0.90 to 3.46 Ga. These granites, space-related with calcalkaline
 637 diorites and gabbros, were interpreted by Solá et al. (2008) as the result of
 638 underplating and temporal storage of mantle-derived magmas as a potential source for
 639 the intrusive “orogenic melts” during Early Palaeozoic extension.

640 Some samples from (i) the Central Iberian Zone, such as VI-3 (Leucogneiss subgroup)
 641 and PORT2 and PORT15 (Granite subgroup); (ii) the eastern Pyrenees, such as 99338
 642 (G1 subgroup) and 100786 samples (Casemí subgroup); and (iii) the Sardinian CS5,
 643 CS8 and CC5 samples (Upper Ordovician Orthogneiss subgroup) display anomalous
 644 T_{DM} values and $^{147}\text{Sm}/^{144}\text{Nd}$ ratios > 0.17 (Table 2; Fig. 14), a character relatively
 645 common in some felsic rocks (DePaolo, 1988; Martínez et al., 2011). According to
 646 Stern et al. (2012), these values should not be considered, but a possible explanation
 647 for these high ratios may be related to the M-type tetrad effect (e.g., Irber, 1999;
 648 Monecke et al., 2007; Ibrahim et al., 2015), which affects REE fractionation in highly
 649 evolved felsic rocks due to the interaction with hydrothermal fluids. This process can be
 650 reflected as an enrichment of Sm related to Nd. Other authors, however, explain this
 651 enrichment as a result of both magmatic evolution (e.g., McLennan, 1994; Pan, 1997)
 652 and weathering processes after exhumation (e.g., Masuda and Akagi, 1989; Takahasi
 653 et al., 2002).

654 In the granites of the southern Central Iberian Zone and the volcanic rocks of
 655 Sardinia, positive values in $\varepsilon\text{Nd}_{(\text{t})}$ could be interpreted as a more primitive nature of
 656 their parental magmas, even though the samples with highest T_{DM} values are those
 657 that display higher $^{147}\text{Sm}/^{144}\text{Nd}$ ratios (> 0.17 ; Table 2).

658 The volcanic rocks of the Central Iberian Zone display some differences following a
 659 N-S transect, being $\varepsilon\text{Nd}_{(\text{t})}$ values **less variable** in the north ($\varepsilon\text{Nd}_{(\text{t})}$: –4.0 to –5.0) than in

660 the south ($\epsilon\text{Nd}_{(\text{t})}$: -1.6 to -5.5). The isotopic signature of the Urra volcaniclastic rocks is
661 compatible with magmas derived from young crustal rocks, with intermediate to felsic
662 igneous compositions (Solá et al., 2008). The volcanic rocks of the northern Central
663 Iberian Zone could be derived from old crustal rocks (Montero et al., 2007). The
664 isotopic composition of the granitoids from the southern Central Iberian Zone has more
665 primitive characters than those of the northern Central Iberian Zone, suggesting
666 different sources for both sides (Talavera et al., 2013). OSS shows lower inheritance
667 patterns, more primitive Sr–Nd isotopic composition than other rocks of the Ollo de
668 Sapo suite, and an age some 15 m.y. younger than most meta-igneous rocks of the
669 Sanabria region (Montero et al., 2009), likely reflecting a greater mantle involvement in
670 its genesis (Díez-Montes et al., 2008).

671 According to Talavera et al. (2013), the Cambro–Ordovician rocks of the Galicia-
672 Trás-os-Montes Zone schistose area and the magmatic rocks of the northern Central
673 Iberian Zone are contemporary. Both metavolcanic and metagranitic rocks almost
674 share the same isotopic compositions.

675 The Upper Ordovician orthogneisses from the Occitan Domain show very little
676 variation in $\epsilon\text{Nd}_{(\text{t})}$ values (-3.5 to -4.0), typical of magmas derived from young crustal
677 rocks. The variation in TDM values is also small (1.4 to 1.8 Ga) indicating similar
678 crustal residence times to other rock groups.

679 In Sardinia, $\epsilon\text{Nd}_{(\text{t})}$ values present a greater variation (-1.6 to -3.3), but they are also
680 included in the typical continental crustal range. As noted above, abnormal TDM values
681 (between 1.2 to 4.5 Ga) may be due to post-magmatic hydrothermal alteration
682 processes.

683

684 5. Geodynamic setting

685

686 In the Iberian Massif, the Ediacaran–Cambrian transition was marked by
687 paraconformities and angular discordances indicating the passage from Cadomian

688 volcanic arc to rifting conditions. The axis of the so-called Ossa-Morena Rift lies along
689 the homonymous Zone (Quesada, 1991; Sánchez-García et al., 2003, 2008, 2010)
690 close to the remains of the Cadomian suture (Murphy et al., 2006). Rifting conditions
691 were accompanied by a voluminous magmatism that changed from peraluminous acid
692 to bimodal (Sánchez-García et al., 2003, 2008, 2016, 2019). Some authors (Álvaro et
693 al., 2014; Sánchez-García et al., 2019) propose that this rift resulted from a SW-to-NE
694 inward migration, toward innermost parts of Gondwana, of rifting axes from the Anti-
695 Atlas in Morocco to the Ossa-Morena Zone in the Iberian Massif. According to this
696 proposal the rifting developed later (in Cambro–Ordovician times) in the Iberian,
697 Armorican and Bohemian massifs.

698 The Furongian–Ordovician transition to drifting conditions is associated, in the
699 Iberian Massif, Occitan Domain, Pyrenees and Sardinia, with a stepwise magmatic
700 activity contemporaneous with the record of the Toledanian and Sardic unconformities.
701 These, related to neither metamorphism nor penetrative deformations, are linked to
702 uplift, erosion and irregularly distributed mesoscale deformation that gave rise to
703 angular unconformities up to 90°. The time span involved in these gaps is similar (22
704 m.y. in the Iberian Massif, 16–23 m.y. in the Pyrenees and 18 m.y. in Sardinia). This
705 contrasts with the greater time span displayed by the magmatic activity (30–45 m.y.),
706 which started before the unconformity formation (early Furongian in the Central Iberian
707 Zone vs. Floian in the Pyrenees, Occitan Domain and Sardinia), continued during the
708 unconformity formation (Furongian and early Tremadocian in the Central Iberian Zone
709 vs. Floian–Darriwilian in the Pyrenees, Occitan Domain and Sardinia), and ended
710 during the sealing of the uplifted and eroded palaeorelief (Tremadocian–Floian
711 volcanioclastic rocks at the base of the Armorican Quartzite in the Central Iberian Zone
712 vs. Sandbian–Katian volcanic rocks at the lowermost part of the Upper Ordovician
713 successions in the Pyrenees, Occitan Domain and Sardinia; Gutiérrez-Alonso et al.,
714 2007, 2016; Navidad et al., 2010; Martínez et al., 2011; Álvaro et al., 2016; Martí et al.,
715 2019). In the Pyrenees, Upper Ordovician magmatism and sedimentation coexist with

716 normal faults controlling marked thickness changes of the basal Upper Ordovician
717 succession and cutting the lower part of this succession, the Sardic unconformity and
718 the underlying Cambro–Ordovician sequence (Puddu et al., 2018, 2019).

719 Although the Toledanian and Sardic Phases reflect similar geodynamic conditions in
720 two distinct palaeogeographic areas, at present forming the western and eastern
721 branches of the Variscan Ibero-Armorian Arc, they display different peaks in magmatic
722 activity with a minor chronological overlapping (Fig. 3). This may reflect a SW-to-NE
723 “zip-like” propagation of the latest Ediacaran–Terreneuvian rifting axes in the so-called
724 **Atlas-Ossa Morena Rift.**

725

726 *Toledanian Phase*

727

728 The Early Ordovician (Toledanian) magmatism of the Central Iberian Zone evolved to a
729 typical passive-margin setting, with geochemical features dominated by acidic rocks,
730 peraluminous and rich in K, and lacking any association with basic or intermediate
731 rocks. Some of the orthogneisses of the Galicia-Trás-os-Montes Zone basal and
732 allochthonous complex units share these same patterns. This fact has been interpreted
733 by some authors as a basin environment subject to important episodes of crustal
734 extension (Martínez-Catalán et al., 2007; Díez-Montes et al., 2010). In contrast,
735 Villaseca et al. (2016) interpreted this absence as evidence against rifting conditions,
736 though the absence of contemporary basic magmatism may be explained by the partial
737 fusion of a thickened crust, through recycling of Neoproterozoic crustal materials. The
738 thrust of a large metasedimentary sequence could generate dehydration and
739 metasomatism of the rocks above this sequence, triggering partial fusion at different
740 levels, although the increase in peraluminosity with the basicity of the orthogneisses is
741 against any AFC process involving mantle materials. However, this increase in
742 peraluminosity with the basicity has not been revealed in the samples studied above.
743 Following Villaseca et al.’s (2016) model, a flat subduction of the southern part of the

744 Central Iberian Zone would have taken place under its northern prolongation, whereas
745 the reflection of such a subduction is not evident in the field. The calc-alkaline signature
746 of this magmatism has also been taken into account as proof of its relationship with
747 volcanic-arc environments (Valverde-Vaquero and Dunning, 2000). However, calc-
748 alkaline features may be also interpreted as a result of a variable degree of continental
749 crustal contamination and/or previously enriched mantle source (Sánchez-García et al.,
750 2003, 2008, 2016, 2019; Díez-Montes et al., 2010). Finally, other granites not
751 considered here of Tremadocian age have been reported in the southern Central
752 Iberian Zone, such as the Oledo massif and the Beira Baixa-Central Extremadura,
753 which display a I-type affinity (Antunes et al., 2009; Rubio Ordóñez et al., 2012). These
754 granites could represent different sources for the Ordovician magmatism in the Central
755 Iberian Zone.

756 Sánchez-García et al. (2019) have proposed that the anomaly that produced the
757 large magmatism throughout the Iberian Massif could have migrated from the rifting
758 axis to inwards zones and the acid, peraluminous, K-rich rocks of Mid Ordovician in
759 age should represent the initial stages of a new rifting pulse, resembling the
760 peraluminous rocks of the Early Rift Event *sensu* Sánchez-García et al. (2003) from the
761 Cambrian Epoch 2 of the Ossa-Morena Rift.

762 In the parautochthon of the Galicia-Trás-os-Montes Zone, the appearance of
763 tholeiitic and alkaline-peralkaline magmatism in the Mid Ordovician would signal the
764 first steps toward extensional conditions (Díez Fernández et al., 2012; Dias da Silva et
765 al., 2016). In the Montagne Noire and the Mouthoumet massifs contemporaneous
766 tholeiitic lavas indicate a similar change in the tectonic regimen (Álvaro et al., 2016).
767 This gradual change in geodynamic conditions is also marked by the appearance of
768 rocks with extensional characteristics in some of subgroups considered here, such as
769 the Central Iberian Zone (San Sebastián orthogneisses), eastern Pyrenees (Casemí
770 orthogneisses, and G1), volcanic rocks of the Occitan Domain, and the orthogneises
771 and volcanic rocks from Sardinia.

772

773 *Sardic Phase*

774

775 In the eastern Pyrenees, two peaks of **Ordovician** magmatic activity **are observed**
776 (Casas et al., 2019). Large Lower–Middle Ordovician peraluminous granite bodies are
777 known representing the protoliths of numerous gneissic bodies with laccolithic
778 morphologies. In the Canigó massif, the Upper Ordovician granite bodies (protholiths of
779 Cadí, Casemí, G1) are encased in sediments of the Canaveilles and Jujols groups.
780 During this time span, there was generalized uplift and erosion that culminated with the
781 onset of the Sardic unconformity. The Sardic Phase was succeeded by an extensional
782 **interval** related to the formation of normal faults affecting the pre–unconformity strata
783 (Puddu et al., 2018, 2019). The volcanic arc signature can be explain by crustal
784 recycling (Navidad et al., 2010; Casas et al., 2010; Martínez et al., 2011), as in the
785 case of the Toledanian Phase in the Central Iberian Zone, although, according to
786 Casas et al. (2019), the Pyrenees and the Catalan Coastal Ranges were probably
787 fringing the Gondwana margin in a different position than that occupied by the Iberian
788 Massif. As a whole, the Ordovician magmatism in the Pyrenees lasted about 30 m.y.,
789 from ca 477 to 446 Ma, in a time span contemporaneous with the formation of the
790 Sardic unconformity ([Fig. 2](#)). Recently, Puddu et al. (2019) proposed that a thermal
791 doming, bracketted between 475 and 450 Ma, **could** have stretched the Ordovician
792 lithosphere. The emersion and denudation of the inherited Cambrian–Ordovician
793 palaeorelief would have given rise to the onset of the Sardic unconformity. According to
794 these authors, thermal doming triggered by hot mafic magma underplating may also be
795 responsible for the late Early–Late Ordovician coeval magmatic activity.

796 In the Occitan Domain, there was a dramatic volcanic event in early Tremadocian
797 times, with the uprising of basin floors and the subsequent effusion of abundant
798 rhyolitic activities under subaerial explosive conditions (Larroque volcanosedimentary
799 Complex in the Montagne Noire, and Davejean acidic volcanic counterpart in the

800 Mouthoumet Massif). Pouclet et al., (2017) interpreted this as a delayed Ollo de Sapo-
801 style outpouring where a massive crustal melting required a rather significant heat
802 supply. Asthenospheric upwelling leading to the interplay of lithospheric doming,
803 continental break-up, and a decompressionally driven mantle melting can explain such
804 a great thermal anomaly. The magmatic products accumulated on the mantle-crust
805 contact would provide enough heat transfer for crustal melting (Huppert and Sparks,
806 1988). Subsequently, a post-Sardic reactivation of rifting conditions is documented in
807 the Cabrières klippe (southern Montagne Noire) and the Mouthoumet massif. There, a
808 Late Ordovician fault-controlled subsidence linked to the record of rift-related tholeiites
809 (Roque de Bandies and Villerouge formations) were contemporaneous with the record
810 of the Hirnantian glaciation (Álvaro et al., 2016). Re-opening of rifting branches
811 (Montagne Noire and Mouthoumet massifs) was geometrically recorded as onlapping
812 patterns and final sealing of Sardic palaeorelief by Silurian and Lower Devonian
813 strata.

814 Sardinia illustrates an almost complete record of the Variscan Belt (Carmignani et
815 al., 1994; Rossi et al., 2009). Some plutonic orthogneises of the Inner Zone belong to
816 this cycle, such as the orthogneises of Golfo Aranci (Giacomini et al., 2006). Gaggero
817 et al. (2012) described three magmatic cycles. The first cycle is well represented in the
818 Sarrabus unit by Furongian-Tremadocian volcanic and subvolcanic interbeds within a
819 terrigenous succession (San Vito Formation) which is topped by the Sardic
820 unconformity. Some plutonic orthogneises of the Inner Zone belong to this cycle, such
821 as the orthogneises of Golfo Aranci (Giacomini et al., 2006) and the PB orthogneiss of
822 Punta Bianca). The second Mid-Ordovician cycle, about 50 m.y. postdating the
823 previous cycle, is of an arc-volcanic type with calc-alkaline affinity and acidic-to-
824 intermediate composition. The acidic metavolcanites are referred in the literature as
825 “porphyroids”, which crop out in the External Nappe Zone and some localities of the
826 Inner Zone. The intermediate to basic derivates are widespread in Central Sardinia
827 (Serra Tonnai Formation). Some plutonic rocks (Mt. Filau orthogneisses and Capo

828 Spartivento) of the second cycle are discussed above. The third cycle consists of
829 alkalic meta-epiclastites interbedded in post-Sandbian strata and metabasites marking
830 the Ordovician/Silurian contact and reflecting rifting conditions. In this work only the first
831 two cycles **are** considered. Giacomini et al. (2006) cite coeval mafic rocks of felsic
832 magmatism of Mid Ordovician age (Cortesogno et al., 2004; Palmeri et al., 2004;
833 Giacomini et al., 2005), although they interpret a subduction scenario of the Hun terrain
834 below Corsica and Sardinia in the Mid Ordovician.

835

836 *Origin of intracrustal siliceous melts*

837

838 In this scenario, the key to generate large volumes of acidic rocks in an intraplate
839 context would be the existence of a lower-middle crust, highly hydrated, in addition to a
840 high heat flow, possibly caused by mafic **melts** (Bryan et al., 2002; Díez-Montes, 2007).
841 This could be the scenario **initiated** by the arrival of a thermal anomaly in a subduction-
842 free area (Sánchez-García et al., 2003, 2008, 2019; Álvaro et al., 2016). The formation
843 of large volumes of intracrustal siliceous melts could act as a viscous barrier,
844 preventing the rise of mafic magmas within volcanic environments, and causing the
845 underplating of these magmas at the contact between the lower crust and the mantle
846 (Huppert and Sparks, 1988; Pankhurst et al., 1998; Bindeman and Valley, 2003). The
847 cooling of these magmas could lead to crustal thickening and in this case, the volcanic
848 arc signature can be explained by crustal recycling (Navidad et al., 2010; Díez-Montes
849 et al., 2010; Martínez et al., 2011).

850 Sánchez-García et al. (2019) have proposed that the anomaly that produced the
851 large magmatism throughout the Iberian Massif could have migrated from the rifting
852 axis to inwards zones and the acid, peraluminous, K-rich rocks of Mid Ordovician in
853 age should represent the initial stages of a new rifting pulse, resembling the
854 peraluminous rocks of the Early Rift Event *sensu* Sánchez-García et al. (2003) from the
855 Cambrian Epoch 2 of the Ossa-Morena Rift. In the parautochthon of the Galicia-Trás-

856 os-Montes Zone, the appearance of tholeiitic and alkaline-peralkaline magmatism in
857 the Mid Ordovician would signal the first steps toward extensional conditions (Díez
858 Fernández et al., 2012; Dias da Silva et al., 2016). In the Montagne Noire and the
859 Mouthoumet massifs contemporaneous tholeiitic lavas indicate a similar change in the
860 tectonic regimen (Álvaro et al., 2016). This change in geodynamic conditions is also
861 marked by the appearance of rocks with extensional characteristics in some of
862 subgroups considered here, such as the Central Iberian Zone (San Sebastián
863 orthogneisses), eastern Pyrenees (Casemí orthogneisses, and G1), volcanic rocks of
864 the Occitan Domain, and the orthogneises and volcanic rocks from Sardinia. In the
865 Pyrenees, Puddu et al. (2019) proposed that a thermal doming, between 475 and 450
866 Ma, should have stretched the Ordovician lithosphere leading to emersion and
867 denudation of a Cambrian–Ordovician palaeorelief, and giving rise to the onset of the
868 Sardic unconformity. According to these authors, thermal doming triggered by hot mafic
869 magma underplating may also be responsible for the late Early–Late Ordovician coeval
870 magmatic activity

871 A major continental break-up, leading to the so-called Tremadocian Tectonic Belt,
872 was suggested by Pouclet et al. (2017), which initiated by upwelling of the
873 asthenosphere and tectonic thinning of the lithosphere. Mantle-derived mafic magmas
874 were underplated at the mantle-crust transition zone and intruded the crust. These
875 magmas provided heat for crustal melting, which supplied the rhyolitic volcanism. After
876 emptying the rhyolitic crustal reservoirs, the underlying mafic magmas finally rose and
877 reached the surface. According to Pouclet et al. (2017), the acidic magmatic output
878 associated with the onset of the Larroque metarhyolites resulted in massive crustal
879 melting requiring a rather important heat supply. Asthenospheric upwelling leading to
880 lithospheric doming, continental break-up, and a decompressional driven mantle
881 melting can explain such a great thermal anomaly. Magmatic products accumulated on
882 the mantle-crust contact providing enough heat transfer for crustal melting.

883

884 **6. Conclusions**

885

886 A geochemical comparison of 231 plutonic and volcanic samples of two major suites,
887 Furongian–Mid Ordovician and Late Ordovician in age, from the Central Iberian and
888 Galicia-Trás-os-Montes Zones of the Iberian Massif and in the eastern Pyrenees,
889 Occitan Domain (Albigeois, Montagne Noire and Mouthoumet massifs) and Sardinia
890 points to a predominance of materials derived from the melting of metasedimentary
891 rocks, peraluminous and rich in SiO_2 and K_2O . The total content in REE is moderate to
892 high. Most felsic rocks display similar chondritic normalized REE patterns, with an
893 enrichment of LREE relative to HREE, which should indicate the involvement of crustal
894 materials in their parental magmas.

895 Zr/TiO_2 , Zr/Nb , Nb/Y and Zr vs. Ga/Al ratios, and REE and εNd values reflect
896 contemporaneous arc and extensional scenarios, which progressed to distinct
897 extensional conditions finally associated with outpouring of mafic tholeiitic-dominant
898 rifting lava flows. Magmatic events are contemporaneous with the formation of the
899 Toledanian (Furongian–Early Ordovician) and Sardic (Early–Late Ordovician)
900 unconformities, related to neither metamorphism nor penetrative deformation. The
901 geochemical and structural framework precludes subduction generated melts reaching
902 the crust in a magmatic arc to back-arc setting. On the contrary, it favours partial
903 melting of sediments and/or granitoids in a continental lower crust triggered by the
904 underplating of hot mafic magmas related to the opening of the Rheic Ocean as a
905 result of asthenospheric upwelling.

906

907 **7. Acknowledgements**

908

909 The authors thank the constructive and useful revisions made by Laura Gaggero
910 (Genoa, Italy) and Jochen Mezger (Fairbanks, USA). This paper is a contribution to
911 projects CGL2017-87631-P and PGC2018-093903-B-C22 from Spanish Ministry of

912 Science and Innovation. We acknowledge support of the publication fee by the CSIC
913 Open Access Publication Support Initiative through its Unit of Information Resources
914 for Research (URICI).

915

916 **Data availability** - All data included in the paper and the Repository Data.

917

918 **Author contributions** - JJA, TSG and JMC: Methodology (Lead), Supervision (Lead),
919 Writing – Original Draft (Lead), Writing – Review & Editing (Lead); CP, ADM, ML & GO:
920 Methodology (Supporting), Supervision (Supporting), Writing – Original Draft
921 (Supporting), Writing – Review & Editing (Supporting).

922

923 **Competing interests** - No competing interests

924

925 **References**

926

- 927 Alabouvette, B., Demange, M., Guérangé-Lozes, J., Ambert, P., 2003. Notice
928 explicative de la carte géologique de Montpellier au 1/250 000. BRGM, Orléans.
- 929 Álvaro, J.J., Vizcaíno, D., 2018. The Furongian break-up (rift-drift) transition in the Anti-
930 Atlas, Morocco. *J. Iberian Geol.* 44, 567–587.
- 931 Álvaro, J.J., Ferretti, F., González-Gómez, C., Serpagli, E., Tortello, M. F., Vecoli, M.,
932 Vizcaíno, D., 2007. A review of the Late Cambrian (Furongian) palaeogeography in
933 the western Mediterranean region, NW Gondwana. *Earth-Sci. Rev.* 85, 47–81.
- 934 Álvaro, J.J., Ezzouhairi, H., Ribeiro, M.L., Ramos, J.F., Solá, A.R., 2008. Early
935 Ordovician volcanism of the Iberian Chains (NE Spain) and its influence on
936 preservation of shell concentrations. *Bull. Soc. géol. France* 179(6), 569–581.
- 937 Álvaro, J.J., Bellido, F., Gasquet, D., Pereira, F., Quesada, C., Sánchez-García, T.,
938 2014a. Diachronism of late Neoproterozoic–Cambrian arc-rift transition of North

- 939 Gondwana: a comparison of Morocco and the Iberian Ossa-Morena Zone. *J. Afr.*
940 *Earth Sci.* 98, 113–132.
- 941 Álvaro, J.J., Bauluz, B., Clausen, S., Devaere, L., Gil Imaz, A., Monceret, E., Vizcaíno,
942 D., 2014b. Stratigraphy of the Cambrian–Lower Ordovician volcanosedimentary
943 complexes, northern Montagne Noire, France. *Stratigraphy* 11, 83–96.
- 944 Álvaro, J.J., Colmenar, J., Monceret, E., Pouclet, A., Vizcaíno, D., 2016. Late
945 Ordovician (post-Sardic) rifting branches in the North Gondwanan Montagne Noire
946 and Mouthoumet massifs of southern France. *Tectonophysics* 681, 111–123.
- 947 Álvaro, J.J., Casas, J.M., Clausen, S., Quesada, C., 2018. Early Palaeozoic
948 geodynamics in NW Gondwana. *J. Iberian Geol.* 44, 551–565.
- 949 Álvaro, J.J., Cortijo, I., Jensen, S., Lorenzo, S., Palacios, T., Pieren, A., 2019. Updated
950 stratigraphic framework and biota of the Ediacaran and Terreneuvian in the Alcudia-
951 Toledo Mountains of the Central Iberian Zone, Spain. *Est. Geol.* 75(2), e093.
- 952 Antunes, I.M.H.R., Neiva, A.M.R., Silva, M.M.V.G., Corfu, F., 2009. The genesis of I-
953 and S-type granitoid rocks of the Early Ordovician Oledo pluton, Central Iberian
954 Zone (central Portugal). *Lithos* 111, 168–185.
- 955 Arthaud, F., 1970. Etude tectonique et microtectonique comparée de deux domaines
956 hercyniens: les nappes de la Montagne Noire (France) et l'anticlinorium de
957 l'Iglesiente (Sardaigne). PhD, Univ. Montpellier.
- 958 Ayora, C., 1980. Les concentrationes métal·liques de la Vall de Ribes. PhD, Univ.
959 Barcelona.
- 960 Ballèvre, M., Fourcade S., Capdevila, R., Peucat, J.J., Cocherie, A., Mark Fanning, C.,
961 2012. Geochronology and geochemistry of Ordovician felsic volcanism in the
962 Southern Armorican Massif (Variscan belt, France): Implications for the breakup of
963 Gondwana. *Gondwana Res.* 21, 1019–1036.
- 964 Barca, S., 1991. Phénomènes de resédimentation et flysch hercynien à faciès Culm
965 dans le “synclinal du Sarrabus” (SE de la Sardaigne, Italie). *C. R. Acad. Sci., Paris*
966 313(2), 1051–1057.

- 967 Barca, S., Cherchi, A., 2004. Regional geological setting. In: Barca, S., Cherchi, A.
968 (eds.), Sardinian Palaeozoic Basement and its Meso–Cainozoic Cover (Italy). 32nd
969 Int. Geol. Congress. Field Trip Guide Book–P39 (5), 3–8.
- 970 Barca, S., Carmignani, L., Maxia, M., Oggiano, G., Pertusati, P.C., 1986. The Geology
971 of Sarrabus. In: Guide-Book to the Excursion on the Paleozoic Basement of Sardinia
972 (Carmignani, L., Cocoza, T., Ghezzo, C., Pertusati, P.C., Ricci, C.A., eds.). IGCP
973 NewsL., Spec. Iss. 5, 51–60.
- 974 Barca, S., Cocoza, T., Del Rio, M., Pillola, G.L., Pittau Demelia, P., 1987. Datation de
975 l'Ordovicien inférieur par *Dictyonema flabelliforme* et acritarches dans la partie
976 supérieure de la formation “cambrienne” de Cabitza (SW de la Sardaigne, Italie):
977 conséquences géodynamiques. C. R. Acad. Sci., Paris 305(2), 1109–1113.
- 978 Barca, S., Del Rio, M., Pittau Demelia, P., 1988. New geological and stratigraphical
979 data and discovery of Lower Ordovician acritarchs in the San Vito Sandstone of the
980 Genn'Argolas Unit (Sarrabus, Southeastern Sardinia). Riv. It. Paleontol. Stratigr. 94,
981 339–360.
- 982 Bea, F., Montero, P., Talavera, C., Zinger, T., 2006. A revised Ordovician age for the
983 Miranda do Douro orthogneiss, Portugal. Zircon U–Pb ion-microprobe and LA–
984 ICPMS dating. Geol. Acta 4, 395–401.
- 985 Bea, F., Montero, P., González Lodeiro, F., Talavera, C., 2007. Zircon inheritance
986 reveals exceptionally fast crustal magma generation processes in Central Iberia
987 during the Cambro–Ordovician. J. Petrol. 48, 2327–2339
- 988 Bé Mézème, E., 2005. Contribution de la géochronologie U–Th–Pb sur monazite à la
989 compréhension de la fusion crustale dans la chaîne Hercynienne française et
990 implication géodynamique. PhD, Univ. Orléans.
- 991 Bindeman, I.N., Valley, J.W., 2003. Rapid generation of both high- and low- $\delta^{18}\text{O}$, large-
992 volume silicic magmas at the Timber Mountain/Oasis Valley caldera complex,
993 Nevada. Geol. Soc. Am. Bull. 115(5), 581–595.

- 994 Boni, M., 1986. The Permo-Triassic vein and paleokarst ores in southwest Sardinia:
995 contribution of fluid inclusion studies to their genesis and paleoenvironment. *Mineral.*
996 *Deposita* 21, 53–62.
- 997 Boni, M., Koeppel, V., 1985. Ore-lead isotope pattern from the Iglesiente-Sulcis area
998 (SW Sardinia) and the problem of remobilization of metals. *Mineral. Deposita* 20,
999 185–193.
- 1000 Bryan, S.E., Riley, T.R., Jerram, D.A., Stephens, Ch.J., Leat, Ph.T., 2002. Silicic
1001 volcanism: An undervalued component of large igneous provinces and volcanic
1002 rifted margins. In: *Volcanic Rifted Margins* (Menzies, M.A., Klemperer, S.L., Ebinger,
1003 C.J., Baker, J., eds.). *Geol. Soc. Am., Spec. Pap.* 362, 99–120.
- 1004 Calvet, P., Lapierre, H., Chavet, J., 1988. Diversité du volcanisme Ordovicien dans la
1005 région de Pierrefitte (Hautes Pyrénées): rhyolites calco-alcalines et basaltes
1006 alcalins. *C. R. Acad. Sci., Paris* 307, 805–812.
- 1007 Calvino, F., 1972. Note Illustrative della Carta Geologica d'Italia, Foglio 227 –
1008 Muravera. Servizio Geologico d'Italia, Roma, 60 p.
- 1009 Carmignani, L., Cocozza, T., Ghezzo, C., Pertusati, P.C., Ricci, C.A., 1986. Guide-
1010 book to the Excursion on the Palaeozoic Basement of Sardinia. IGCP Project no. 5,
1011 Newsl. Spec. Iss., 1–102.
- 1012 Carmignani, L., Pertusati, P.C., Barca, S., Carosi, R., Di Pisa, A., Gattiglio, M., et al.,
1013 1992. Struttura della Catena Ercinica in Sardegna. Guida all'escursione del Gruppo
1014 Informali di Geologia Strutturale in Sardegna, 24–29 (Maggio), 1–177.
- 1015 Carmignani, L., Carosi, R., Di Pisa, A., Gattiglio, M., Musumeci, G., Oggiano, G. et al.,
1016 1994. The Hercynian chain in Sardinia (Italy). *Geodin. Acta* 7, 31–47.
- 1017 Carmignani, L., Oggiano, G., Barca, S., Conti, P., Salvadori, I., Eltrudis, A. et al. 2001.
1018 Geologia della Sardegna. Note illustrative della Carta Geologica della Sardegna a
1019 scala 1:200.000. *Memorie Descrittive della Carta Geologica d'Italia*, Servizio
1020 Geologico 60, 1–283. Instituto Poligrafico e Zecca dello Stato, Roma.

- 1021 Caron, C., Lancelot, J., Omenetto, P., Orgeval, J.J., 1997. Role of the Sardic tectonic
1022 phase in the metallogenesis of SW Sardinia (Iglesiente): lead isotope evidence.
1023 European J. Miner. 9, 1005–1016.
- 1024 Casas, J.M., 2010. Ordovician deformations in the Pyrenees: new insights into the
1025 significance of pre–Variscan ('sardic') tectonics. Geol. Mag. 147, 674–689.
- 1026 Casas, J.M., Fernández, O., 2007. On the Upper Ordovician unconformity in the
1027 Pyrenees: New evidence from the La Cerdanya area. Geol. Acta 5, 193–198.
- 1028 Casas, J.M., Murphy, J.B. 2018. Unfolding the arc: the use of pre-orogenic constraints
1029 to assess the evolution of the Variscan belt in Western Europe. Tectonophysics 736,
1030 47–61.
- 1031 Casas, J.M., Palacios, T., 2012. First biostratigraphical constraints on the pre–Upper
1032 Ordovician sequences of the Pyrenees based on organic-walled microfossils. C. R.
1033 Geosci. 344, 50–56.
- 1034 Casas, J.M., Castiñeiras, P., Navidad, M., Liesa, M., Carreras, J., 2010. New insights
1035 into the Late Ordovician magmatism in the Eastern Pyrenees: U–Pb SHRIMP zircon
1036 data from the Canigó massif. Gondwana Res. 17, 317–324.
- 1037 Casas, J.M., Álvaro, J.J., Clausen, S., Padel, M., Puddu, C., Sanz-López, J., Sánchez-
1038 García, T., Navidad, M., Castiñeiras, P., Liesa, M., 2019. Palaeozoic basement of
1039 the Pyrenees. In: The Geology of Iberia: A Geodynamic Approach (Quesada, C.,
1040 Oliveira, J.T., eds.). Regional Geology Reviews, vol. 2, 229–259. Springer,
1041 Heidelberg.
- 1042 Castiñeiras, P., Villaseca, C., Barbero, L., Martín-Romera, C., 2008a. SHRIMP U–Pb
1043 zircon dating of anatexis in high-grade migmatite complexes of Central Spain:
1044 implications in the Hercynian evolution of Central Iberia. Int. J. Earth Sci. 97, 35–50.
- 1045 Castiñeiras, P., Navidad, M., Liesa, M., Carreras, J., Casas, J.M., 2008b. U–Pb zircon
1046 ages (SHRIMP) for Cadomian and Lower Ordovician magmatism in the Eastern
1047 Pyrenees: new insights in the pre–Variscan evolution of the northern Gondwana
1048 margin. Tectonophysics 46, 228–239.

- 1049 Castro, A., García-Casco, A., Fernández, C., Corretgé, L.G., Moreno-Ventas, I., Gerya,
1050 T., Löw, I., 2009. Ordovician ferrosilicic magmas: experimental evidence for
1051 ultrahigh temperaturas affecting a metagreywacke source. *Gondwana Res.* 16, 622–
1052 632
- 1053 Charles, N., Faure, M., Chen, Y., 2008. The emplacement of the Montagne Noire axial
1054 zone (French Massif Central): New insights from petro-textural, geochronological
1055 and AMS studies. *22ème Réunion des Sciences de la Terre, Nancy*, 155.
- 1056 Charles, N., Faure, M., Chen, Y., 2009. The Montagne Noire migmatitic dome
1057 emplacement (French Massif Central): New insights from petrofabric and AMS
1058 studies. *J. Struct. Geol.* 31, 1423–1440.
- 1059 Clariana, P., Valverde-Vaquero, P., Rubio-Ordóñez, A., Beranoaguirre, A., García-
1060 Sansegundo, J., 2018. Pre–Variscan tectonic events and Late Ordovician
1061 magmatism in the Central Pyrenees: U–Pb age and Hf in zircon isotopic signature
1062 from subvolcanic sills in the Pallaresa massif. *J. Iberian Geol.* 44, 589–601.
- 1063 Cocco, F., Funedda, A., 2011. New data on the pre–Middle Ordovician deformation in
1064 SE Sardinia: a preliminary note. *Rend. online Soc. Geol. It.* 15, 34–36.
- 1065 Cocco, F., Funedda, A., 2017. The Sardic Phase: field evidence of Ordovician tectonics
1066 in SE Sardinia. *Italy. Geol. Mag.* 156, 25–38.
- 1067 Cocco, F., Oggiano, G. Funedda, A., Loi, A., Casini, L., 2018. Stratigraphic, magmatic
1068 and structural features of Ordovician tectonics in Sardinia (Italy): a review. *J. Iberian
1069 Geol.* 44, 619–639.
- 1070 Cocherie, A., 2003. Datation avec le SHRIMP II du métagranite oeillé du Somail-
1071 Montagne Noire. *C. R. technique ANA–ISO/NT, BRGM*.
- 1072 Cocherie, A., Baudin, T., Guerrot, C., Autran, A., Fanning, M.C., Laumonier, B., 2005.
1073 U–Pb zircon (ID–TIMS and SHRIMP) evidence for the early Ordovician intrusion of
1074 metagranites in the late Proterozoic Canaveilles Group of the Pyrenees and the
1075 Montagne Noire (France). *Bull. Soc. géol. France* 176, 269–282.

- 1076 Cortesogno, L., Gaggero, L., Oggiano, G., Paquette, J.L., 2004. Different tectono-
1077 thermal evolution paths in eclogitic rocks from the Axial Zone of the Variscan Chain
1078 in Sardinia (Italy) compared with the Ligurian Alps. *Ofioliti* 29, 125–144.
- 1079 Costamagna, L.G., Elter, F.M., Gaggero, L., Mantovani, F., 2016. Contact
1080 metamorphism in Middle Ordovician arc rocks (SW Sardinia, Italy): New
1081 paleogeographic constraints. *Lithos* 264, 577–593.
- 1082 Cruciani, G., Franceschelli, M., Musumeci, G., Spano, M.E., Tiepolo, M., 2013. U–Pb
1083 zircon dating and nature of metavolcanics and metarkoses from the Monte Grighini
1084 Unit: new insights on Late Ordovician magmatism in the Variscan belt in Sardinia,
1085 Italy. *Int. J. Earth Sci.* 102, 2077–2096.
- 1086 Cruciani, G., Franceschelli, M., Puxeddu, M., Tiepolo, M., 2018. Metavolcanics from
1087 Capo Malfatano, SW Sardinia, Italy: New insight on the age and nature of
1088 Ordovician volcanism in the Variscan foreland zone. *Geol. J.* 53(4), 1573–1585.
- 1089 Demange, M., 1999. Evolution tectonique de la Montagne noire: un modèle en
1090 transpression. *C. R. Acad. Sci., Paris* 329, 823–829.
- 1091 Demange, M., Guérangé-Lozes, J., Guérangé, B., 1996. Notice explicative de la feuille
1092 de Lacaune (987) au 1:50 000. BRGM, Orléans.
- 1093 Denèle, Y., Barbe, P., Deloule, E., Pelleter, E., Olivier, Ph., Gleizes, G., 2009. Middle
1094 Ordovician U–Pb age of the Aston and Hospitalet orthogneissic laccoliths: their role
1095 in the Variscan evolution of the Pyrenees. *Bull. Soc. géol. France* 180, 209–221.
- 1096 DePaolo, D.J., 1981. Neodymium isotopes in the Colorado Front Range and crust-
1097 mantle evolution in the Proterozoic. *Nature* 291, 193–196.
- 1098 DePaolo, D.J., 1988. Neodymium isotope geochemistry. An introduction. *Minerals and*
1099 *Rocks Series* 20, 1–187. Springer-Verlag, Berlin.
- 1100 DePaolo, D.J., Wasserburg, G.J., 1976. Nd isotopic variations and petrogenetic
1101 models. *Geophys. Res. Lett.* 3(5), 249–252.

- 1102 Dias da Silva Í., 2014. Geología de las Zonas Centro Ibérica y Galicia-Tras-os-Montes
1103 en la parte oriental del Complejo de Morais, Portugal/España. Serie Nova Terra 45,
1104 1–424.
- 1105 Dias da Silva, I., Valverde-Vaquero, P., González-Clavijo, E., Díez-Montes, A.,
1106 Martínez-Catalán, J.R., 2012. Structural and stratigraphical significance of U–Pb
1107 ages from the Saldanha and Mora volcanic complexes (NE Portugal, Iberian
1108 Variscides). Géol. France 1, 105–106.
- 1109 Dias da Silva Í., Valverde-Vaquero, P., González Clavijo E., Díez-Montes A., Martínez
1110 Catalán J.R., 2014. Structural and stratigraphical significance of U–Pb ages from the
1111 Mora and Saldanha volcanic complexes (NE Portugal, Iberian Variscides). In:
1112 Schulmann, K., Martínez Catalán, J. R., Lardeaux, J. M., Janousek, V., Oggiano, G.,
1113 (eds.), The Variscan Orogeny: Extent, Timescale and the Formation of the
1114 European Crust. Geol. Soc., London, Spec. Publ. 405, 115–135.
- 1115 Dias da Silva, I., Díez Fernández, R., Díez Montes, A., González Clavijo, E., Foster,
1116 D.A., 2016. Magmatic evolution in the N-Gondwana margin related to the opening of
1117 the Rheic Ocean – evidence from the Upper Parautochthon of the Galicia-Trás-os-
1118 Montes Zone and from the Central Iberian Zone (NW Iberian Massif). Int. J. Earth
1119 Sci. 105, 1127–1151.
- 1120 Díaz-Alvarado, J., Fernández, C., Chichorro, M., Castro, A., Pereira, M.F., 2016.
1121 Tracing the Cambro–Ordovician ferrosilicic to calc-alkaline magmatic association in
1122 Iberia by *in situ* U–Pb SHRIMP zircon geochronology (Gredos massif, Spanish
1123 Central System batholith). Tectonophysics 681, 95–110.
- 1124 Díez Fernández, R., Castiñeiras, P., Gómez Barreiro, J., 2012. Age constraints on
1125 Lower Paleozoic convection system: Magmatic events in the NW Iberian Gondwana
1126 margin. Gondwana Res. 21, 1066–1079.
- 1127 Díez-Montes, A., 2007. La Geología del Dominio “Ollo de Sapo” en las Comarcas de
1128 Sanabria y Terra do Bolo. PhD, Univ. Salamanca. Laboratorio Xelóxico de Laxe,
1129 Serie Nova Terra no. 34, A Coruña.

- 1130 Díez Montes, A., Martínez Catalán, J.R., Bellido Mulas, F., 2010. Role of the Ollo de
1131 Sapo massive felsic volcanism of NW Iberia in the Early Ordovician dynamics of
1132 northern Gondwana. *Gondwana Res.* 17, 363–376.
- 1133 Di Pisa, A., Gattiglio, M., Oggiano, G., 1992. Pre-Hercynian magmatic activity in the
1134 nappe zone (internal and external) of Sardinia: evidence of two within plate basaltic
1135 cycles. In: Contributions to the Geology of Italy with Special Regard to the Paleozoic
1136 Basements (Carmignani, L., Sassi, F.P., eds.). *Newsl. IGCP* 276, 107–116.
- 1137 Echtler, H., Malavieille, J., 1990. Extensional tectonics, basement uplift and Stephano–
1138 Permian collapse basin in a late Variscan metamorphic core complex (Montagne
1139 Noire, southern Massif Central). *Tectonophysics* 177, 125–138.
- 1140 El Khor, A., Schmidt , S.Th., Ballèvre, M., Ulianov, A., Bruguier, O., 2012. Discovery of
1141 an albite gneiss from the Ile de Groix (Armorican Massif, France): geochemistry and
1142 LA-ICP-MS U–Pb geochronology of its Ordovician protolith. *Int. J. Earth Sci.* 101,
1143 1169–1190.
- 1144 Engel,W., Feist, R., Franke,W., 1980. Le Carbonifère anté-stéphanien de la Montagne
1145 Noire: rapports entre mise en place des nappes et sédimentation. *Bull. BRGM* 2,
1146 341–389.
- 1147 Farias, P., Ordoñez-Casado, B., Marcos, A., Rubio-Ordóñez, A., Fanning, C.M., 2014.
1148 U–Pb zircon SHRIMP evidence for Cambrian volcanism in the Schistose Domain
1149 within the Galicia-Trás-os-Montes Zone (Variscan Orogen, NW Iberian Peninsula).
1150 *Geol. Acta* 12(3), 209–218.
- 1151 Faure, M., Ledru, P., Lardeaux, J.M., Matte, P., 2004. Paleozoic orogenies in the
1152 French Massif Central. A cross section from Béziers to Lyon. 32nd Int. Geol.
1153 Congress Florence (Italy), Field-trip guide book, 40 p.
- 1154 Feist, R., Galtier, J., 1985. Découverte de flores d'âge namurien probable dans le
1155 flysch à olistolithes de Cabrières (Hérault). Implications sur la durée de la
1156 sédimentation synorogénique dans la Montagne Noire (France Méridionale). *C. R.*
1157 *Acad. Sci., Paris* 300, 207–212.

- 1158 Franz, L., Romer, R.L., 2007. Caledonian high-pressure metamorphism in the Strona-
1159 Ceneri-Zone (Southern Alps of southern Switzerland and northern Italy). *Swiss J.*
1160 *Geosci.* 100, 457–467.
- 1161 Friedl, G., Finger, F., Paquette, J.L., von Quadt, A., McNaughton, N.J., Fletcher, I.R.,
1162 2004. Pre-Variscan geological events in the Austrian part of the Bohemian Massif
1163 deduced from U-Pb zircon ages. *Int. J. Earth Sci.* 93, 802–823
- 1164 Funedda, A., Oggiano, G., 2009. Outline of the Variscan basement of Sardinia. In: The
1165 Silurian of Sardinia. Volume in Honour of Enrico Serpagli (Corradini, C., Ferretti, A.,
1166 Štorch, P., eds.). *Rend. Soc. Paleontol. It.* 3, 23–35.
- 1167 Gaggero L., Oggiano G., Funedda A., Buzzi L., 2012. Rifting and arc-related Early
1168 Paleozoic volcanism along the North Gondwana margin: Geochemical and
1169 geological evidence from Sardinia (Italy). *J. Geol.* 120, 273–292.
- 1170 García-Arias, M., Díez-Montes, A., Villaseca, C., Blanco-Quintero, I.F. 2018. The
1171 Cambro-Ordovician Ollo de Sapo magmatism in the Iberian Massif and its Variscan
1172 evolution: A review. *Earth-Sci. Rev.* 176, 345–372.
- 1173 Gèze, B., 1949. Etude géologique de la Montagne Noire et des Cévennes
1174 méridionales. *Mém. Soc. géol. France* 62, 1–215.
- 1175 Giacomini, F., Bomparola, R.M., Ghezzo, C., 2005. Petrology and geochronology of
1176 metabasites with eclogite facies relics from NE Sardinia: constraints for the
1177 Palaeozoic evolution of Southern Europe. *Lithos* 82, 221–248
- 1178 Giacomini, F., Bomparola, R.M., Ghezzo, C., Guldbansen, H., 2006. The geodynamic
1179 evolution of the Southern European Variscides: constraints from the U/Pb
1180 geochronology and geochemistry of the lower Palaeozoic magmatic-sedimentary
1181 sequences of Sardinia (Italy). *Contrib. Miner. Petr.* 152, 19–42.
- 1182 Guérangé-Lozes, J., Alabouvette, B., 1999. Notice explicative, *Carte géol. France* (1/50
1183 000), feuille Saint-Sernin-sur-Rance (960). BRGM, Orléans, 84 p.

- 1184 Guérangé-Lozes, J., Guérangé, B., Mouline, M.P., Delsahut, B., 1996. Notice
1185 explicative, Carte géol. France (1/50 000), feuille Réalmont (959). BRGM, Orléans,
1186 78 p.
- 1187 Guitard, G., 1970. Le métamorphisme hercynien mésozonal et les gneiss oeillés du
1188 masif du Canigou (Pyrénées orientales). Mém. BRGM 63, 1–353.
- 1189 Gutiérrez-Alonso, G., Fernández-Suárez, J., Gutiérrez-Marco, J.C., Corfu, F., Murphy,
1190 J.B., Suárez Martínez, S., 2007. U–Pb depositional age for the upper Barrios
1191 Formation (Armorican Quartzite facies) in the Cantabrian zone of Iberia: implications
1192 for stratigraphic correlation and paleogeography. In: The Evolution of the Rheic
1193 Ocean: from Avalonian–Cadomian Active Margin to Alleghenian–Variscan Collision
1194 (Linnemann, R.D., Nance, P., Kraft, G.Z., eds.). Geol. Soc. Am., London, 287–296.
- 1195 Gutiérrez-Alonso, G., Gutiérrez-Marco, J.C., Fernández-Suárez, J., Bernárdez, E.,
1196 Corfu, F., 2016. Was there a super-eruption on the Gondwanan coast 477 Ma ago?
1197 Tectonophysics 681, 85–94.
- 1198 Gutiérrez-Marco, J.C., Robardet, M., Rábano, I., Sarmiento, G., San José Lancha,
1199 M.A., Herranz Araújo, P., Pieren Vidal, A., 2002. Ordovician. In: The Geology of
1200 Spain, (Gibbons, W., Moreno, T., eds.), 31–49, Geological Society, London
- 1201 Gutiérrez-Marco, J.C., Piçarra, J.M., Meireles, C.A., Cázar, P., García-Bellido, D.C.,
1202 Pereira, Z. et al., 2019. Early Ordovician–Devonian Passive margin stage in the
1203 Gondwanan units of the Iberian massif. In: The Geology of Iberia: A Geodynamic
1204 Approach (Quesada, C., Oliveira, J.T., eds.). Regional Geology Reviews, vol. 2, 75–
1205 98. Springer, Heidelberg.
- 1206 Hartevelt, J.J.A., 1970. Geology of the upper Segre and Valira valleys, central
1207 Pyrenees, Andorra/Spain. Leid. Geol. Meded. 45, 167–236.
- 1208 Helbing, H., Tiepolo, M., 2005. Age determination of Ordovician magmatism in NE
1209 Sardinia and its bearing on Variscan basement evolution. J. Geol. Soc. 162, 689–
1210 700.

- 1211 Huppert, H.E., Sparks, R.S.J., 1988. The generation of granitic magmas by intrusion of
1212 basalt into continental crust. *J. Petrol.* 29, 599–624.
- 1213 Ibrahim, M.E., El-Kalioby, B.A., Aly, G.M., El-Tohamy, A.M., Watanabe, K., 2015.
1214 Altered granitic rocks, Nusab El Balgum Area, Southwestern Desert, Egypt.
1215 Mineralogical and geochemical aspects of REEs. *Ore Geol. Rev.* 70, 252–261.
- 1216 Irber, W., 1999. The lanthanide tetrad effect and its correlation with K/Rb, Eu/Eu*,
1217 Sr/Eu, Y/Ho, and Zr/Hf of evolving peraluminous granite suites. *Geochim.
1218 Cosmochim. Acta* 63, 489–508.
- 1219 Jégouzo, P., Peucat, J.J., Audren, C., 1986. Caractérisation et signification
1220 géodynamique des orthogneiss calco-alcalins d'âge ordovicien de Bretagne
1221 méridionale. *Bull. Soc. géol. France* 2, 839–848.
- 1222 Kröner, A., Willner, A.P., 1998. Time of formation and peak of Variscan HP-HT
1223 metamorphism of quartz-feldspar rocks in the central Erzgebirge, Saxony, Germany.
1224 *Contrib. Mineral. Petrol.* 132, 1–20
- 1225 Lancelot, J., Allegret, A., Iglesias Ponce de León, M., 1985. Outline of Upper
1226 Precambrian and Lower Paleozoic evolution of the Iberian Peninsula according to
1227 U-Pb dating of zircons. *Earth Planet. Sci. Lett.* 74, 325–337.
- 1228 Laske, R., Bechstädt, T., Boni, M., 1994. The post-Sardic Ordovician series. In:
1229 Sedimentological, stratigraphical and ore deposits field guide of the autochthonous
1230 Cambro-Ordovician of Southeastern Sardinia (Bechstädt, T., Boni, M., eds.).
1231 Memorie descrittive della carta geologica d'Italia 48, 115–146.
- 1232 Leat, P.T., Jackson, S.E., Thorpe, R.S., Stillman, C.J., 1986. Geochemistry of bimodal
1233 basalt-subalkaline/peralkaline rhyolite provinces within the Southern British
1234 Caledonides. *J. Geol. Soc.* 143, 259–273.
- 1235 Le Corre, C., Auvray, B., Ballèvre, M., Robardet, M., 1991. Le Massif Armorican. *Sci.
1236 Géol., Bull.* 44, 31–103.
- 1237 Lentz, D., 1996. U, Mo and REE mineralization in late-tectonic granite pegmatites,
1238 south-west Grenville Province, Canada. *Ore Geol. Rev.* 11, 197–227.

- 1239 Leone, F., Hamman, W., Laske, R., Serpagli, E., Villas, E., 1991. Lithostratigraphic
1240 units and biostratigraphy of the post-Sardic Ordovician sequence in south-west
1241 Sardinia. *Boll. Soc. Paleontol. It.* 30, 201–235.
- 1242 Leone, F., Ferretti, A., Hammann, W., Loi, A., Pillola, G.L., Serpagli, E., 2002. A
1243 general view of the post-Sardic Ordovician sequence from SW Sardinia. *Rend. Soc.*
1244 *Paleontol. It.* 1, 51–68.
- 1245 Lescuyer, J.L., Cocherie, A., 1992. Datation sur monozircons des métadacites de
1246 Séries: arguments pour un âge protérozoïque terminal des “schistes X” de la
1247 Montagne Noire (Massif central français). *C. R. Acad. Sci., Paris (sér. 2)* 314, 1071–
1248 1077.
- 1249 Liesa, M., Carreras, J., Castiñeiras, P., Casas, J.M., Navidad, M., Vilà, M., 2011. U–Pb
1250 zircon age of Ordovician magmatism in the Albera Massif (Eastern Pyrenees). *Geol.*
1251 *Acta* 9, 1–9.
- 1252 Linnemann, U., Gehmlich, M., Tichomirowa, M., Buschmann, B., Nasdala, L., Jonas, P.
1253 et al. 2000. From Cadomian subduction to early Palaeozoic rifting: the evolution of
1254 Saxo-Thuringia at the margin of Gondwana in the light of single zircon
1255 geochronology and basin development (Central European Variscides, Germany). In:
1256 Orogenic Processes: Quantification and Modelling in the Variscan Belt (Franke, W.,
1257 Haak, V., Oncken, O., Tanner, D., eds.). *Geol. Soc., London, Spec. Publ.* 179, 131–
1258 153.
- 1259 Loi, A., Dabard, M.P., 1997. Zircon typology and geochemistry in the palaeogeographic
1260 reconstruction of the Late Ordovician of Sardinia (Italy). *Sediment. Geol.* 112, 263–
1261 279.
- 1262 Loi, A., Barca, S., Chauvel, J.J., Dabard, M.P., Leone, F., 1992. Analyse de la
1263 sédimentation post-phase sarde les dépôts initiaux à placers du SE de la Sardaigne.
1264 *C. R. Soc. géol. France (sér. 2)* 315, 1357–1364.
- 1265 López-Sánchez, M.A., Iriondo, A., Marcos, A., Martínez, F.J., 2015. A U–Pb zircon age
1266 (479 ± 5 Ma) from the uppermost layers of the Ollo de Sapo Formation near Viveiro

- 1267 (NW Spain): implications for the duration of rifting-related Cambro–Ordovician
1268 volcanism in Iberia. *Geol. Mag.* 152, 341–350.
- 1269 Ludwig, K.R., Turi, B., 1989. Paleozoic age of the Capo Spartivento Orthogneiss,
1270 Sardinia, Italy. *Chem. Geol.* 79, 147–153.
- 1271 Margalef, A., Castiñeiras, P., Casas, J.M., Navidad, M., Liesa, M., Linnemann, U.,
1272 Hofmann, M., Gärtner, A., 2016. Detrital zircons from the Ordovician rocks of the
1273 Pyrenees: Geochronological constraints and provenance. *Tectonophysics* 681, 124–
1274 134.
- 1275 Marini, F., 1988. “Phase“ sarde et distension ordovicienne du domaine sud-varisque,
1276 effets de point chaud? Une hypothèse fondée sur les données nouvelles du
1277 volcanisme albigeois. *C. R. Acad. Sci., Paris (sér. 2)* 306, 443–450.
- 1278 Martí, J., Muñoz, J.A., Vaquer, R., 1986. Les roches volcaniques de l’Ordovicien
1279 supérieur de la région de Ribes de Freser-Rocabruna (Pyrénées catalanes):
1280 caractères et signification. *C. R. Acad. Sci., Paris* 302, 1237–1242.
- 1281 Martí, J., Solari, L., Casas, J.M., Chichorro, M., 2019. New late Middle to early Late
1282 Ordovician U–Pb zircon ages of extension-related felsic volcanic rocks in the
1283 Eastern Pyrenees (NE Iberia): tectonic implications. *Geol. Mag.* 156(10), 1783–
1284 1792.
- 1285 Martínez, F., Iriondo, A., Dietsch, C., Aleinikoff, J.N., Peucat, J.J., Cirès, J., Reche, J.,
1286 Capdevila, R., 2011. U–Pb SHRIMP–RG zircon ages and Nd signature of lower
1287 Paleozoic rifting-related magmatism in the Variscan basement of the Eastern
1288 Pyrenees. *Lithos* 127, 10–23.
- 1289 Martínez Catalán, J.R., Arenas, R., Díaz García, F., Gómez Barreiro, J., González
1290 Cuadra, P., Abati, J. et al. 2007. Space and time in the tectonic evolution of the
1291 northwestern Iberian Massif. Implications for the comprehension of the Variscan
1292 belt. In: 4–D Framework of Continental Crust (Hatcher, R.D.Jr., Carlson, M.P.,
1293 McBride, J.H., Martínez Catalán, J.R., eds.). *Geol. Soc. Am., Mem.* 200, 403–423.

- 1294 Martini, I.P., Tongiorgi, M., Oggiano, G., Cocozza, T., 1991. Ordovician alluvial fan to
1295 marine shelf transition in SW Sardinia, Western Mediterranean Sea: tectonically
1296 ("Sardic" phase") influenced clastic sedimentation. *Sediment. Geol.* 72, 97–115.
- 1297 **Masuda, A., Akagi, T., 1989. Lanthanide tetrad effect observed in leucogranites from**
1298 **China. *Geochem. J.* 23, 245–253.**
- 1299 McDougall, N., Brenchley, P.J., Rebelo, J.A., Romano, M., 1987. Fans and fan deltas –
1300 precursors to the Armorican Quartzite (Ordovician) in western Iberia. *Geol. Mag.*
1301 124, 347–359.
- 1302 **McLennan, S.M., 1994. Rare earth element geochemistry and the "tetrad" effect.**
1303 ***Geochim.Cosmochim. Acta* 58, 2025–2033.**
- 1304 Mezger, J., Gerdes, A., 2016. Early Variscan (Visean) granites in the core of central
1305 Pyrenean gneiss domes: implications from laser ablation U–Pb and Th–Pb studies.
1306 *Gondwana Res.* 29, 181–198.
- 1307 Mingram, B., Kröner, A., Hegner, E., Krentz, O., 2004. Zircon ages, geochemistry, and
1308 Nd isotopic systematics of pre–Variscan orthogneisses from the Erzgebirge, Saxony
1309 (Germany), and geodynamic interpretation. *Int. J. Earth Sci.* 93, 706–727.
- 1310 Monecke, T., Dulski, P., Kempe, U., 2007. Origin of convex tetrads in rare earth
1311 element patterns of hydrothermally altered siliceous igneous rocks from the
1312 Zinnwald Sn–W deposit, Germany. *Geochim. Cosmochim. Acta* 71, 335–353.
- 1313 Montero, P., Bea, F., González-Lodeiro, F., Talavera, C., Whitehouse, M.J., 2007.
1314 Zircon ages of the metavolcanic rocks and metagranites of the Ollo de Sapo Domain
1315 in central Spain: implications for the Neoproterozoic to Early Palaeozoic evolution of
1316 Iberia. *Geol. Mag.* 144, 963–976.
- 1317 Montero, P., Talavera, C., Bea, F., Lodeiro, F.G., Whitehouse, M.J., 2009. Zircon
1318 geochronology of the Ollo de Sapo Formation and the age of the Cambro–
1319 Ordovician rifting in Iberia. *J. Geol.* 117, 174–191.

- 1320 Murphy, J.B., Gutiérrez-Alonso, G., Nance, R.D., Fernández-Suárez, J., Keppie, J.D.,
1321 Quesada, C. et al., 2006. Origin of the Rheic Ocean: rifting along a Neoproterozoic
1322 suture? *Geology* 34, 325–328.
- 1323 Nance, R.D., Gutiérrez-Alonso, G., Keppie, J.D., Linnemann, U., Murphy, J.B.,
1324 Quesada, C. et al., 2010. Evolution of the Rheic Ocean. *Gondwana Res.* 17, 194–
1325 222.
- 1326 Navidad, M., Castiñeiras, P., 2011. Early Ordovician magmatism in the northern
1327 Central Iberian Zone (Iberian Massif): new U–Pb (SHRIMP) ages and isotopic Sr–
1328 Nd data. 11th ISOS, Alcalá de Henares, May 2011.
- 1329 Navidad, M., Castiñeiras, P., Casas, J.M., Liesa, M., Fernández-Suárez, J., Barnolas,
1330 A., Carreras, J., Gil-Peña, I., 2010. Geochemical characterization and isotopic ages
1331 of Caradocian magmatism in the northeastern Iberia: insights into the Late
1332 Ordovician evolution of the northern Gondwana margin. *Gondwana Res.* 17, 325–
1333 337.
- 1334 Navidad, M., Castiñeiras, P., Casas, J.M., Liesa, M., Belousova, E., Proenza, J.,
1335 Aiglsperger, T., 2018. Ordovician magmatism in the Eastern Pyrenees: Implications
1336 for the geodynamic evolution of northern Gondwana. *Lithos* 314–315, 479–496.
- 1337 Neiva, A.M.R., Williams, I.S., Ramos, J.M.F., Gomes, M.E.P., Silva, M.M.V.G.,
1338 Antunes, I.M.H.R., 2009. Geochemical and isotopic constraints on the petrogenesis
1339 of Early Ordovician granodiorite and Variscan two-mica granites from the Gouveia
1340 area, central Portugal. *Lithos* 111, 186–202.
- 1341 Oggiano, G., Gaggero, L., Funedda, A., Buzzi, L., Tiepolo, M., 2010. Multiple early
1342 Paleozoic volcanic events at the northern Gondwana margin: U–Pb age evidence
1343 from the southern Variscan branch (Sardinia, Italy). *Gondwana Res.* 17, 44–58.
- 1344 Padel, M., Álvaro, J.J., Clausen, S., Guillot, F., Poujol, M., Chichorro, M., Monceret, E.,
1345 Pereira, M.F., Vizcaíno, D., 2017. U–Pb laser ablation ICP–MS zircon dating across
1346 the Ediacaran–Cambrian transition of the Montagne Noire, southern France. *C. R.
1347 Geosci.* 349, 380–390.

- 1348 Padel, M., Clausen, S., Álvaro, J.J., Casas, J.M., 2018. Review of the Ediacaran–
1349 Lower Ordovician (pre-Sardic) stratigraphic framework of the Eastern Pyrenees,
1350 southwestern Europe. *Geol. Acta* 16, 339–355
- 1351 Palme, H., O'Neill, H.S.C., 2004. Cosmochemical estimates of mantle composition. In:
1352 *Treatise on Geochemistry 2* (Holland, H.D., Turekian, K.K., eds.), 1–38. Elsevier–
1353 Pergamon, Oxford.
- 1354 Palmeri, R., Fanning, M., Franceschelli, M., Memmi, I., Ricci, C.A., 2004. SHRIMP
1355 dating of zircons in eclogite from the Variscan basement in northeastern Sardinia
1356 (Italy). *N. Jb. Miner., Mh.* 6, 275–288.
- 1357 Pan, Y., 1997. Controls on the fractionation of isovalent trace elements in magmatic
1358 and aqueous systems: evidence from Y/Ho, Zr/Hf, and lanthanide tetrad effect – a
1359 discussion of the article by M. Bau, 1996. *Contrib. Mineral. Petrol.* 128, 405–408.
- 1360 Pankhurst, R.J., Rapela, C.W., Saavedra, J., Baldo, E., Dahlquist, J., Pascua, I.,
1361 Fanning, C.M., 1998. The Famatinian magmatic arc in the central Sierras
1362 Pampeanas, and Early to Middle Ordovician continental arc on the Gondwana
1363 margin. In: *The Proto-Andean Margin of Gondwana* (Pankhurst, R.J., Rapela, C.E.,
1364 eds.). Geol. Soc., London, Spec. Publ. 142, 343–367.
- 1365 Pavanetto, P., Funedda, A., Northrup, C. J., Schmitz, M., Crowley, J., Loi, A., 2012.
1366 Structure and U–Pb zircon geochronology in the Variscan foreland of SW Sardinia,
1367 Italy. *Geol. J.* 47, 426–445.
- 1368 Pearce, J.A., 1996. Sources and settings of granitic rocks. *Episodes* 19, 120–125.
- 1369 Pearce, J.A., Harris, N.B.W., Tindle, A.G., 1984. Trace element discrimination
1370 diagrams for the tectonic interpretation of granitic rocks. *J. Petrol.* 25, 956–983.
- 1371 Pereira, M.F., Solá, A.R., Chichorro, M., Lopes, L., Gerdes, A., Silva, J.B., 2012. North–
1372 Gondwana assembly, break-up and paleogeography: U–Pb isotope evidence from
1373 detrital and igneous zircons of Ediacaran and Cambrian rocks of SW Iberia.
1374 *Gondwana Res.* 22(3–4), 866–881.

- 1375 Piercey, S.J., 2011. The setting, style, and role of magmatism in the formation of
1376 volcanogenic massive sulphide deposits. *Miner. Deposita* 46, 449–471.
- 1377 Pistis, M., Loi, A., Dabard, M.P., 2016. Influence of relative sea-level variations on the
1378 genesis of palaeoplacers, the examples of Sarrabus (Sardinia, Italy) and the
1379 Armorican Massif (western France). *C. R. Geosci.* 348(2), 150–157.
- 1380 Pillola, G.L., Leone, F., Loi, A., 1998. The Cambrian and Early Ordovician of SW
1381 Sardinia. *Gior. Geol. (ser. 3)*, Spec. Iss. 60, 25–38.
- 1382 Pitra, P., Poujol, M., Den Driessche, J.V., Poilvet, J. C., Paquette, J.L., 2012. Early
1383 Permian extensional shearing of an Ordovician granite: the Saint-Eutrope “C/S-like”
1384 orthogneiss (Montagne Noire, French Massif Central). *C. R. Geosci.* 344, 377–384.
- 1385 Pouclet, A., Álvaro, J.J., Bardintzeff, J.M., Gil Imaz, A., Monceret, E., Vizcaïno D.,
1386 2017. Cambrian–Early Ordovician volcanism across the South Armorican and
1387 Occitan Domains of the Variscan Belt in France: Continental break-up and rifting of
1388 the northern Gondwana margin. *Geosci. Frontiers* 8, 25–64.
- 1389 Puddu, C., Álvaro J.J., Casas, J.M., 2018. The Sardic unconformity and the Upper
1390 Ordovician successions of the Ribes de Freser area, Eastern Pyrenees. *J. Iberian
1391 Geol.* 44, 603–617.
- 1392 Puddu, C., Álvaro, J.J., Carrera, N., Casas, J.M., 2019. Deciphering the Sardic
1393 (Ordovician) and Variscan deformations in the Eastern Pyrenees. *J. Geol. Soc.*
1394 176(6), 1191–1206.
- 1395 Quesada, C., 1991. Geological constraints on the Paleozoic tectonic evolution of
1396 tectonostratigraphic terranes in the Iberian Massif. *Tectonophysics* 185, 225–245.
- 1397 Rabin, M., Trap, P., Carry, N. Fréville, K. Cenki-Tok, B. Lobjoie, C. Gonçalves, P.,
1398 Marquer, D., 2015. Strain partitioning along the anatetic front in the Variscan
1399 Montagne Noire massif (southern French Massif Central). *Tectonics* 34, 1709–1735.
- 1400 Robert, J. F. 1980. Étude géologique et métallogénique du val de Ribas sur le versant
1401 espagnol des Pyrénées catalanes. PhD, Univ. Franche-Comté.

- 1402 Robert, J.F., Thiebaut, J., 1976. Découverte d'un volcanisme acide dans le Caradoc de
1403 la région de Ribes de Freser (Prov. de Gérone). *C. R. Acad. Sci., Paris* 282, 2050–
1404 2079.
- 1405 Roger, F., Respaut, J.P., Brunel, M., Matte, Ph., Paquette, J.L., 2004. Première
1406 datation U–Pb des orthogneiss oeillés de la zone axiale de la Montagne Noire (Sud
1407 du Massif central): nouveaux témoins du magmatisme ordovicien dans la chaîne
1408 varisque. *C. R. Geosci.* 336, 19–28
- 1409 Roger, F., Teyssier, C., Respaut, J.P., Rey, P.F., Jolivet, M., Whitney, D.L., Paquette,
1410 J.L., Brunel, M., 2015. Timing of formation and exhumation of the Montagne Noire
1411 double dome, French massif Central. *Tectonophysics* 640–641, 53–69.
- 1412 Rollison, H.R., 1993. *Using Geochemical Data: Evaluation, Presentation, Interpretation.*
1413 Longman Group, London, 352 p.
- 1414 Romão, J., Dunning, G., Marcos, A., Dias, R., Ribeiro, A., 2010. O lacólito granítico de
1415 Mação-Penhascoso: idade e as suas implicações (SW da Zona Centro-Ibérica). *e-*
1416 *Terra* 16, 1–4.
- 1417 Rossi, P., Oggiano, G., Cocherie, A., 2009. A restored section of the “southern
1418 Variscan realm” across the Corsica-Sardinia microcontinent. *C. R. Geosci.* 34, 224–
1419 238.
- 1420 Rubio-Ordóñez, A., Valverde-Vaquero, P., Corretgé, L. G., Cuesta-Fernández, A.,
1421 Gallastegui, G., Fernández-González, M., Gerdes, A., 2012. An Early Ordovician
1422 tonalitic-granodioritic belt along the Schistose-Greywacke Domain of the Central
1423 Iberian Zone (Iberian Massif, Variscan Belt). *Geol. Mag.* 149, 927–939.
- 1424 Rudnick, R.L., Gao, S., 2003. Composition of the Continental Crust. In: *Treatise on*
1425 *Geochemistry* (Holland, H.D., Turekian, K.K., eds.), vol. 3, 1–64. Elsevier–
1426 Pergamon, Oxford.
- 1427 Sánchez-García, T., Bellido, F., Quesada, C., 2003. Geodynamic setting and
1428 geochemical signatures of Cambrian–Ordovician rift-related igneous rocks (Ossa–
1429 Morena Zone, SW Iberia). *Tectonophysics* 365, 233–255.

- 1430 Sánchez-García, T., Quesada, C., Bellido, F., Dunning, G., González de Tánago, J.,
1431 2008. Two-step magma flooding of the upper crust during rifting: the Early Paleozoic
1432 of the Ossa-Morena Zone (SW Iberia). *Tectonophysics* 461, 72–90.
- 1433 Sánchez-García, T., Bellido, F., Pereira, M.F., Chichorro, M., Quesada, C., Pin, Ch.,
1434 Silva, J.B., 2010. Rift-related volcanism predating the birth of the Rheic Ocean
1435 (Ossa-Morena zone, SW Iberia). *Gondwana Res.* 17, 392–407.
- 1436 Sánchez-García, T., Quesada, C., Bellido, F., Dunning, G.R., Pin, Ch., Moreno-Eiris,
1437 E., Perejón, A., 2016. Age and characteristics of the Loma del Aire unit (SW Iberia):
1438 Implications for the regional correlation of the Ossa-Morena Zone. *Tectonophysics*
1439 681, 58–72.
- 1440 Sánchez-García, T., Chichorro, M., Solá, R., Álvaro, J.J., Díez Montes, A., Bellido, F. et
1441 al. 2019. The Cambrian–Early Ordovician Rift Stage in the Gondwanan Units of the
1442 Iberian Massif. In: *The Geology of Iberia: A Geodynamic Approach* (Quesada, C.,
1443 Oliveira, J.T., eds.). *Regional Geol. Rev.* 1, 27–74.
- 1444 Schaltegger, U., Abrecht, J., Corfu, F., 2003. The Ordovician orogeny in the Alpine
1445 basement: constraints from geochronology and geochemistry in the Aar Massif
1446 (Central Alps). *Schweizerische Miner. Petrogr. Mitteil.* 83, 183–195.
- 1447 Shaw, J., Johnston, S., Gutiérrez-Alonso, G., Weil, A.B., 2012. Oroclines of the
1448 Variscan orogen of Iberia: paleocurrent analysis and paleogeographic implications.
1449 *Earth Planet. Sci. Lett.* 329–330, 60–70.
- 1450 Shaw, J., Gutiérrez-Alonso, G., Johnston, S., Pastor Galán, D., 2014. Provenance
1451 variability along the early Ordovician north Gondwana margin: paleogeographic and
1452 tectonic implications of U–Pb detrital zircon ages from the Armorican Quartzite of
1453 the Iberian Variscan belt. *Geol. Soc. Am. Bull.* 126(5–6), 702–719.
- 1454 Solá, A.R., 2007. Relações Petrogeoquímicas dos Maciços Graníticos do NE
1455 Alentejano. PhD, Univ. Coimbra.
- 1456 Solá, A.R., Pereira, M.F., Williams, I.S., Ribeiro, M.L., Neiva, A.M.R., Montero, P., Bea,
1457 F., Zinger, T., 2008. New insights from U–Pb zircon dating of Early Ordovician

- 1458 magmatism on the northern Gondwana margin: the Urria formation (SW Iberian
1459 Massif, Portugal). *Tectonophysics* 461, 114–129.
- 1460 Stern, R.J., 2002. Crustal evolution in the East African Orogen: a neodymium isotopic
1461 perspective. *J. African Earth Sci.* 34, 109–117.
- 1462 Stille, H., 1939. Bemerkungen betreffend die "Sardische" Faultung und den Ausdruck
1463 "Ophiolitisch". *Zeits. Deuts. Gess. Geowiss.* 91, 771–773.
- 1464 Sun, S.S., McDonough, W.F., 1989. Chemical and isotopic systematics of oceanic
1465 basalts: implications for mantle composition and processes. In: *Magmatism in the*
1466 *Ocean Basins* (Saunders, A.D., Norry, M.J., eds.). *Geol. Soc., Spec. Publ.* 42, 13–
1467 345.
- 1468 Syme, E.C., 1998. Ore-Associated and Barren Rhyolites in the central Flin Flon Belt:
1469 Case Study of the Flin Flon Mine Sequence. Manitoba Energy and Mines, Open File
1470 Report OF98–9, 1–32
- 1471 Takahashi, Y., Yoshida, H., Sato, N., Hama, K., Yusa, Y., Shimizu, H., 2002. W- and
1472 M-type tetrad effects in REE patterns for water-rock systems in the Tono uranium
1473 deposit, central Japan. *Chem. Geol.* 184, 311–335.
- 1474 Talavera, C., 2009. Pre-Variscan magmatism of the Central Iberian Zone: chemical
1475 and isotope composition, geochronology and geodynamic significance. PhD, Univ.
1476 Granada.
- 1477 Talavera, C., Bea F, Montero P., Whitehouse, M., 2008. A revised Ordovician age for
1478 the Sisargas orthogneiss, Galicia (Spain). Zircon U–Pb ion-microprobe and LA–
1479 ICPMS dating. *Geol. Acta* 8, 313–317.
- 1480 Talavera, C., Montero, P., Bea, F., González Lodeiro, F., Whitehouse, M., 2013. U–Pb
1481 Zircon geochronology of the Cambro–Ordovician metagranites and metavolcanic
1482 rocks of central and NW Iberia. *Int. J. Earth. Sci.* 102, 1–23.
- 1483 Taylor, S.R., McLennan, S.M., 1985. *The Continental Crust: Its Composition and*
1484 *Evolution*. Blackwell, London, 312 pp.

- 1485 Teichmüller, R., 1931. Zur Geologie des Thyrrhenisgebietes, Teil 1: Alte und junge
1486 Krustenbewegungen im südlichen Sardinien. Abh. Der wissen. Gess. Göttingen
1487 (Math.-Phys. Kl) 3, 857–950.
- 1488 Teipel, U., Eichhorn, R., Loth, G., Rohrmüller, J., Höll, R., Kennedy, A., 2004. U–Pb
1489 SHRIMP and Nd isotopic data from the western Bohemian Massif (Bayerischer
1490 Wald, Germany): Implications for Upper Vendian and Lower Ordovician magmatism.
1491 Int. J. Earth Sci. 93, 782–801.
- 1492 Thompsom, M.D., Grunow, A.M., Ramezani, J., 2010. Cambro–Ordovician
1493 paleogeography of the Southeastern New England Avalon Zone: Implications for
1494 Gondwana breakup. Geol. Soc. Am. Bull. 122, 76–88.
- 1495 Tichomirowa, M., Berger, H.J., Koch, E.A., Belyatski, B., Götze, J., Kempe, U.,
1496 Nasdala, L., Schaltegger, U., 2001. Zircon ages of high-grade gneisses in the
1497 Eastern Erzgebirge (Central European Variscides) – constraints on origin of the
1498 rocks and Precambrian to Ordovician magmatic events in the Variscan foldbelt.
1499 Lithos 56, 303–332.
- 1500 Tichomirowa, M., Sergeev, S., Berger, H.J., Leonhardt, D., 2012. Inferring protoliths of
1501 high-grade metamorphic gneisses of the Erzgebirge using zirconology,
1502 geochemistry and comparison with lower-grade rocks from Lusatia (Saxothuringia,
1503 Germany). Contrib. Mineral. Petrol. 164, 375–396.
- 1504 Valverde-Vaquero, P., Dunning, G.R., 2000. New U–Pb ages for Early Ordovician
1505 magmatism in Central Spain. J. Geol. Soc. London 157, 15–26.
- 1506 Valverde-Vaquero, P., Marcos, A., Farias, P., Gallastegui, G., 2005. U–Pb dating of
1507 Ordovician felsic volcanism in the Schistose Domain of the Galicia-Trás-os-Montes
1508 Zone near Cabo Ortegal (NW Spain). Geol. Acta 3, 27–37.
- 1509 Valverde-Vaquero, P., Farias, P., Marcos, A., Gallastegui, G., 2007. U–Pb dating of
1510 Siluro–Ordovician volcanism in the Verín synform (Orense, Schistose Domain,
1511 Galicia-Trás-os-montes Zone). Geogaceta 41, 247–250.

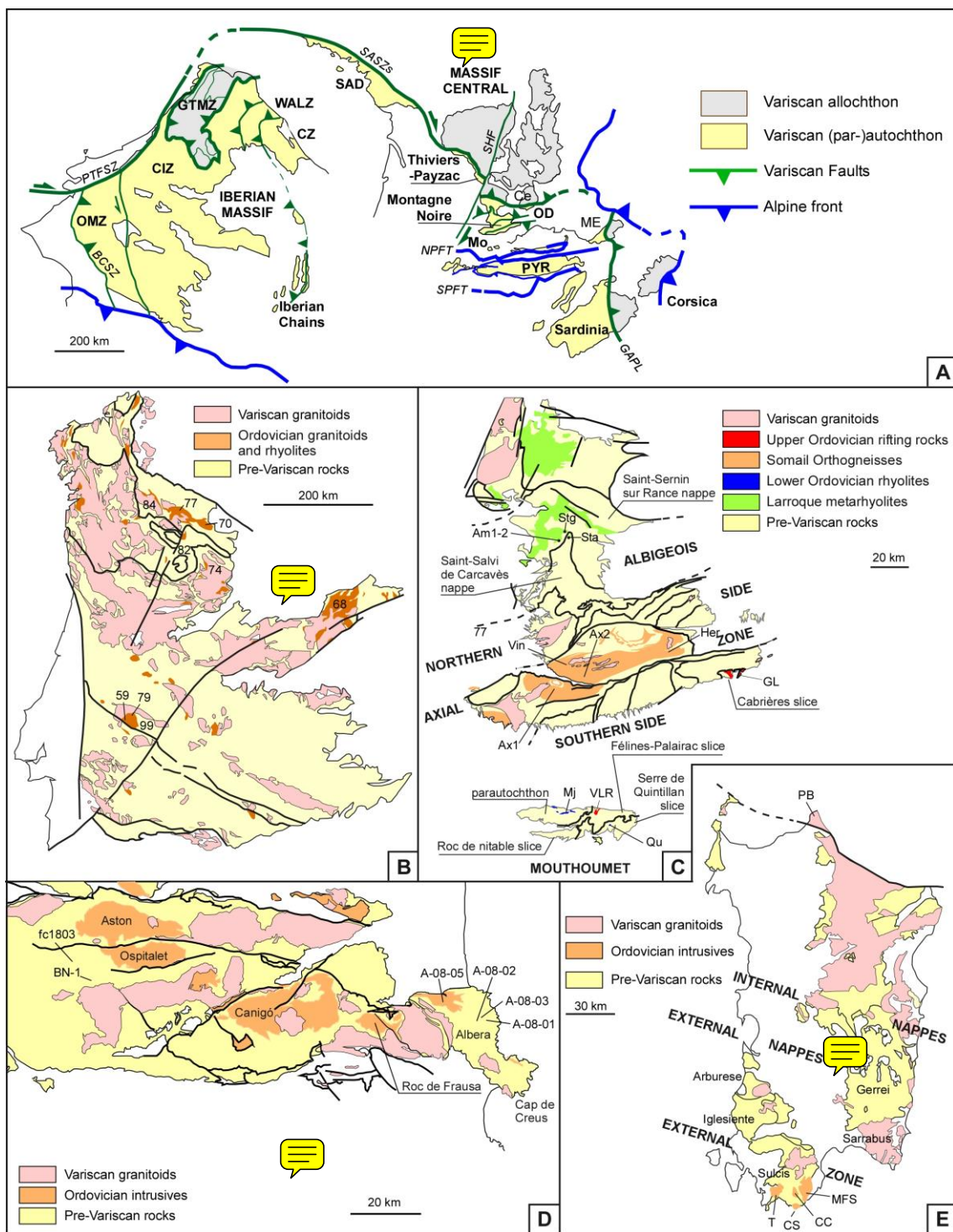
- 1512 Vilà, M., Pin, C., Enrique, P., Liesa, M., 2005. Telescoping of three distinct magmatic
1513 suites in an orogenic setting: Generation of Hercynian igneous rocks of the Albera
1514 Massif (Eastern Pyrenees). *Lithos* 83, 97–127.
- 1515 Villaseca, C., Castiñeiras, P., Orejana, D., 2013. Early Ordovician metabasites from the
1516 Spanish Central System: A remnant of intraplate HP rocks in the Central Iberian
1517 Zone. *Gondwana Res.* 27, 392–409.
- 1518 Villaseca, C., Merino Martínez, E., Orejana, D., Andersen, T., Belousova, E., 2016.
1519 Zircon Hf signatures from granitic orthogneisses of the Spanish Central System:
1520 Significance and sources of the Cambro–Ordovician magmatism in the Iberian
1521 Variscan Belt. *Gondwana Res.* 34, 60–83.
- 1522 Von Quadt, A., 1997. U–Pb zircon and Sr–Nd–Pb whole-rock investigations from the
1523 continental deep drilling (KTB). *Geol. Rundsch.* 86 (suppl.), S258–S271.
- 1524 Von Raumer, J.F., Stampfli, G.M., 2008. The birth of the Rheic Ocean – early
1525 Palaeozoic subsidence patterns and tectonic plate scenarios. *Tectonophysics* 461,
1526 9–20.
- 1527 Von Raumer, J.F., Stampfli, G.M., Borel, G., Bussy, F., 2002. The organization of pre–
1528 Variscan basement areas at the Gondwana margin. *Int. J. Earth Sci.* 91, 35–52.
- 1529 Von Raumer, J.F., Bussy, F., Schaltegger, U., Schulz, B., Stampfli, G., 2013. Pre–
1530 Mesozoic Alpine basements: their place in the European Paleozoic framework.
1531 *Geol. Soc. Am. Bull.* 125, 89–108.
- 1532 Von Raumer, J.F., Stampfli, G.M., Arenas, R., Sánchez Martínez, S., 2015. Ediacaran
1533 to Cambrian oceanic rocks of the Gondwanan margin and their tectonic
1534 interpretation. *Int. J. Earth Sci.* 104, 1107–1121.
- 1535 Whalen, J.B., Currie, K.L., Chappell, B.W., 1987. A-type granites: Geochemical
1536 characteristics, discrimination and petrogenesis. *Contr. Miner. Petrol.* 95, 407–419.
- 1537 Winchester, J.A., Floyd, P.A., 1977. Geochemical discrimination of different magma
1538 series and their differentiation products using immobile elements. *Chem. Geol.* 20,
1539 325–343.

- 1540 Zeck, H.P., Whitehouse, M.J., Ugidos, J.M., 2007. 496 ± 3 Ma zircon ion microprobe
1541 age for pre-Hercynian granite, Central Iberian Zone, NE Portugal (earlier claimed
1542 618 ± 9 Ma). Geol. Mag. 144, 21-31.
- 1543 Zurbiggen, R., 2015. Ordovician orogeny in the Alps – a reappraisal. Int. J. Earth Sci.
1544 104, 335–350.
- 1545 Zurbiggen, R., 2017. The Cenerian orogeny (early Paleozoic) from the perspective of
1546 the Alpine region. Int. J. Earth Sci. 106, 517–529.
- 1547 Zurbiggen, R., Franz, L., Handy, M.R., 1997. Pre-Variscan deformation,
1548 metamorphism and magmatism in the Strona-Ceneri Zone (southern Alps of
1549 northern Italy and southern Switzerland). Schweiz. Miner. Petrograph. Mitteil. 77,
1550 361–380.
- 1551

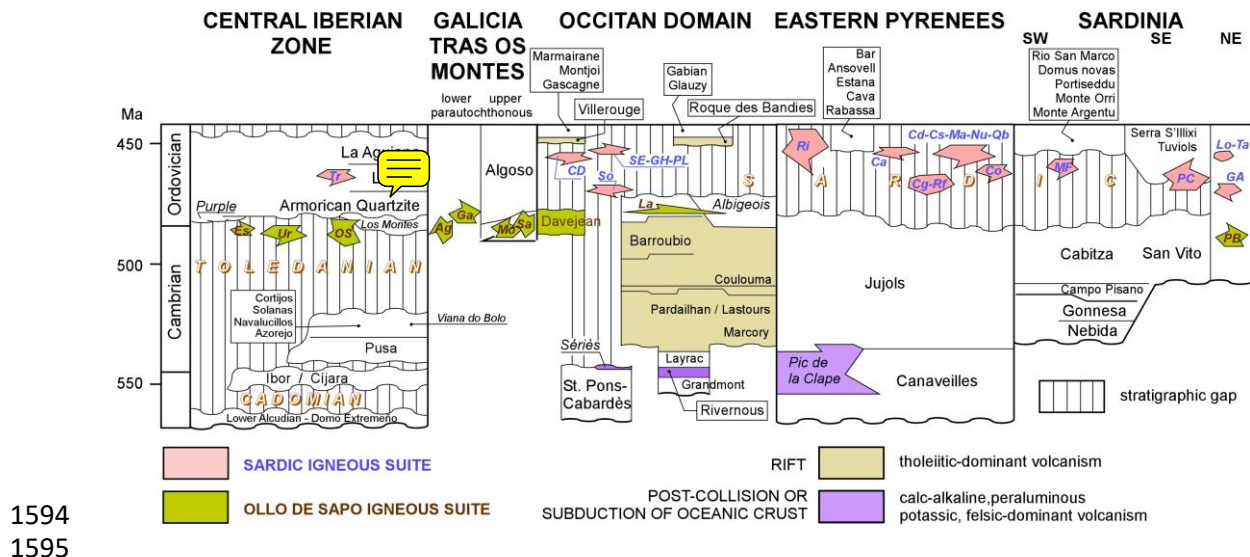
1552 **FIGURE CAPTIONS**

1553

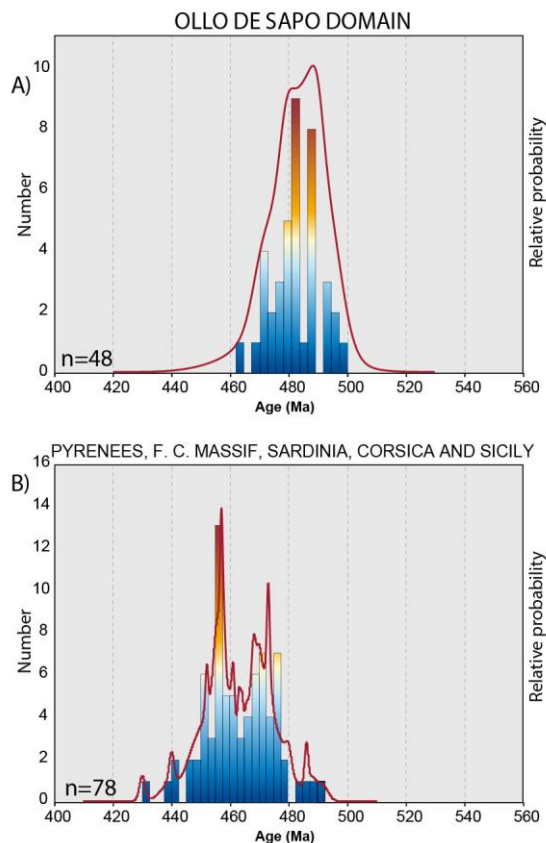
1554 **Figure 1.** A. Reconstruction of the south-western European margin of Gondwana in
1555 Late Carboniferous–Early Permian times; modified from Pouclet et al. (2017). B.
1556 Setting of samples in the Central Iberian and Galicia-Trás-os-Montes zones; 59-
1557 Carrascal, 68- Guadarrama, 70- **Sanabria**, 74- Miranda do Douro, 77- Ollo de Sapo,
1558 79- Portalegre, 82- Saldanha, 84- San Sebastián, 99- Urra, Sa Sanabria; modified from
1559 Sánchez-García et al. (2019). C. Setting of samples in the Montagne Noire and
1560 Mouthoumet massifs; Am1-2 Larroque hamlet (Ambialet), Stg- St.Géraud Sta- St.
1561 André, Mj- Montjoi, Qu- Quintillan, GL- Roque de Bandies, VLR- Villerouge-Termenès,
1562 VIN- Le Vintrou, HER- Gorges d'Héric (Caroux massif), Ax1- S Mazamet (Nore massif),
1563 Ax2 (Rou)- S Rouayroux (Agout massif); modified from Álvaro et al. (2016). D. Setting
1564 of Pyrenean samples; modified from Casas et al. (2019). E. Setting of Sardinian
1565 samples; CS 2,3,4,8- Spartivento Cap, T2- Tuerreda, CC5- Cuile Culurgioni, MF1-
1566 Monte Filau, MFS1-Monte Settiballas, PB- Punta Bianca; modified from Oggiano et al.
1567 (2010).



1570 **Figure 2.** Stratigraphic comparison of the Cambro-Ordovician successions from the
1571 Central Iberian Zone, Galicia Trás-os-Montes Zone, Occitan Domain, Eastern
1572 Pyrenees and Sardinia; modified from Álvaro et al. (2014b, 2016, 2018), Pouclet et al.
1573 (2017) and Sánchez-García et al. (2019); abbreviations: *Ag Agualada*, Ca Campelles
1574 ignimbrites (ca. 455 Ma, Martí et al., 2014), *CD Cadí* gneiss (456 ± 5 Ma, Casas et al.,
1575 2010), *Cg Canigó* gneiss (472–462 Ma, Cocherie et al., 2005; Navidad et al., 2018), *Co*
1576 *Cortalets* metabasite (460 ± 3 Ma, Navidad et al., 2018), *Cs Casemí* gneiss (446 ± 5
1577 and 452 ± 5 Ma, Casas et al., 2010), *Es Estremoz* rhyolites (499 Ma, Pereira et al.,
1578 2012), *Ga Galiñero*, *GA Golfo Aranci* orthogneiss (469 ± 3.7 Ma, Giacomini et al.,
1579 2006), *GH Gorges d'Heric* orthogneiss (450 ± 6 Ma, Roger et al., 2004), *La Larroque*
1580 Volcanic Complex, *Ma Marialles* microdiorite (453 ± 4 Ma, Casas et al., 2010), *Lo Lodè*
1581 orthogneiss (456 ± 14 Ma, Helbing and Tiepolo, 2005), *MF Monte Filau-Capo*
1582 *Spartivento* orthogneiss (449 ± 6 Ma, Ludwing and Turi, 1989; 457.5 ± 0.3 and $458.2 \pm$
1583 0.3 Ma, Pavanetto et al., 2012), *Mo Mora* (493.5 ± 2 Ma, Dias Da Silva et al., 2014), *Nu*
1584 *Núria* gneiss (457 ± 4 Ma, Martínez et al., 2011), *OS Ollo de Sapo* rhyolites and ash-
1585 fall tuff beds (ca. 477 Ma., Gutiérrez-Alonso et al., 2016), *PL Pont de Larn* orthogneiss
1586 (456 ± 3 Ma, Roger et al., 2004), *Qb Queralbs* gneiss (457 ± 5 Ma, Martínez et al.,
1587 2011), *PB Punta Bianca* orthogneiss (broadly Furongian–Tremadocian in age), *PC*
1588 *Porto Corallo* dacites (465.4 ± 1.9 and 464 ± 1 Ma, Giacomini et al., 2006; Oggiano et
1589 al., 2010), *Ri Ribes* granophyre (458 ± 3 Ma, Martínez et al., 2011), *Rf Roc de Frausa*
1590 gneiss (477 ± 4 , 476 ± 5 Ma, Cocherie et al., 2005; Castiñeiras et al., 2008), *So Somail*
1591 orthogneiss (471 ± 4 Ma, Cocherie et al. 2005), *Sa Saldanha* (483.7 ± 1.5 ; Dias da
1592 *Silva*, 2014), *SE Saint Eutrope* gneiss (455 ± 2 Ma, Pitra et al., 2012), *Ta Tanaunella*
1593 orthogneiss 458 ± 7 Ma (Helbing and Tiepolo, 2005), *Tr Turchas* and *Ur Urra* rhyolites.



1596 **Figure 3.** Relative probability plots of the age of the Cambrian–Ordovician magmatism
 1597 for (A) the Ollo de Sapo domain from the Central Iberian Zone; and (B) Pyrenees
 1598 (Guilleries and Gavarres massifs), French Central Massif (including Montagne Noire),
 1599 Sardinia, Corsica and Sicily (n = number of analyses). Data obtained from references
 1600 cited in the text.

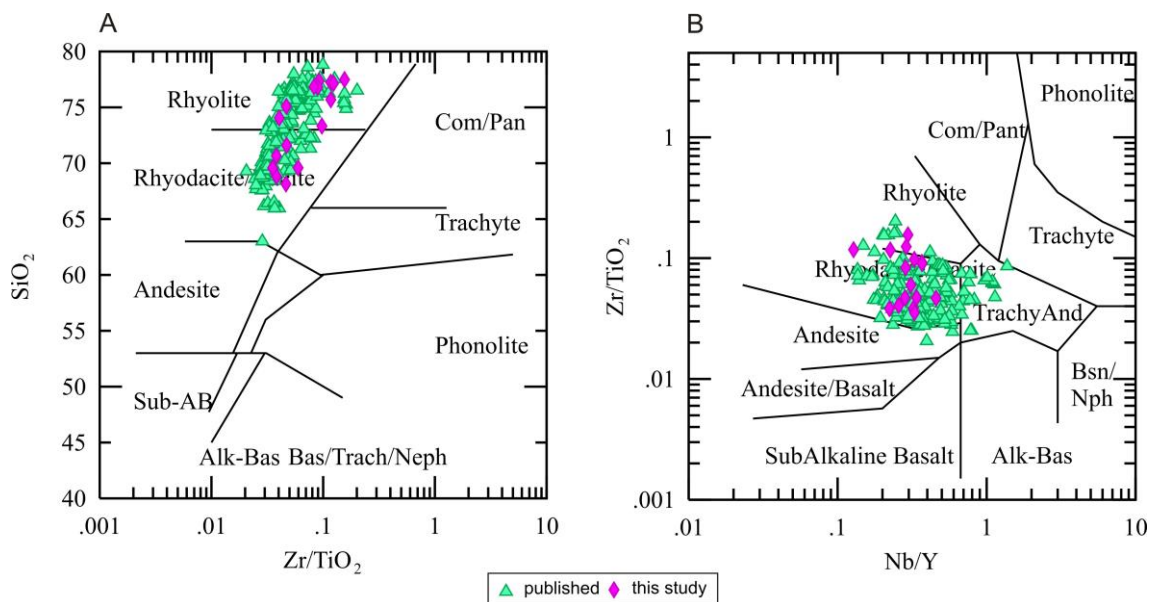


1601

1602

1603 **Figure 4.** SiO_2 vs. Zr/TiO_2 and Zr/TiO_2 vs. Nb/Y plots (Winchester and Floyd, 1977)
 1604 showing the composition of new samples (purple diamonds) and those taken from the
 1605 literature (green triangles).

1606

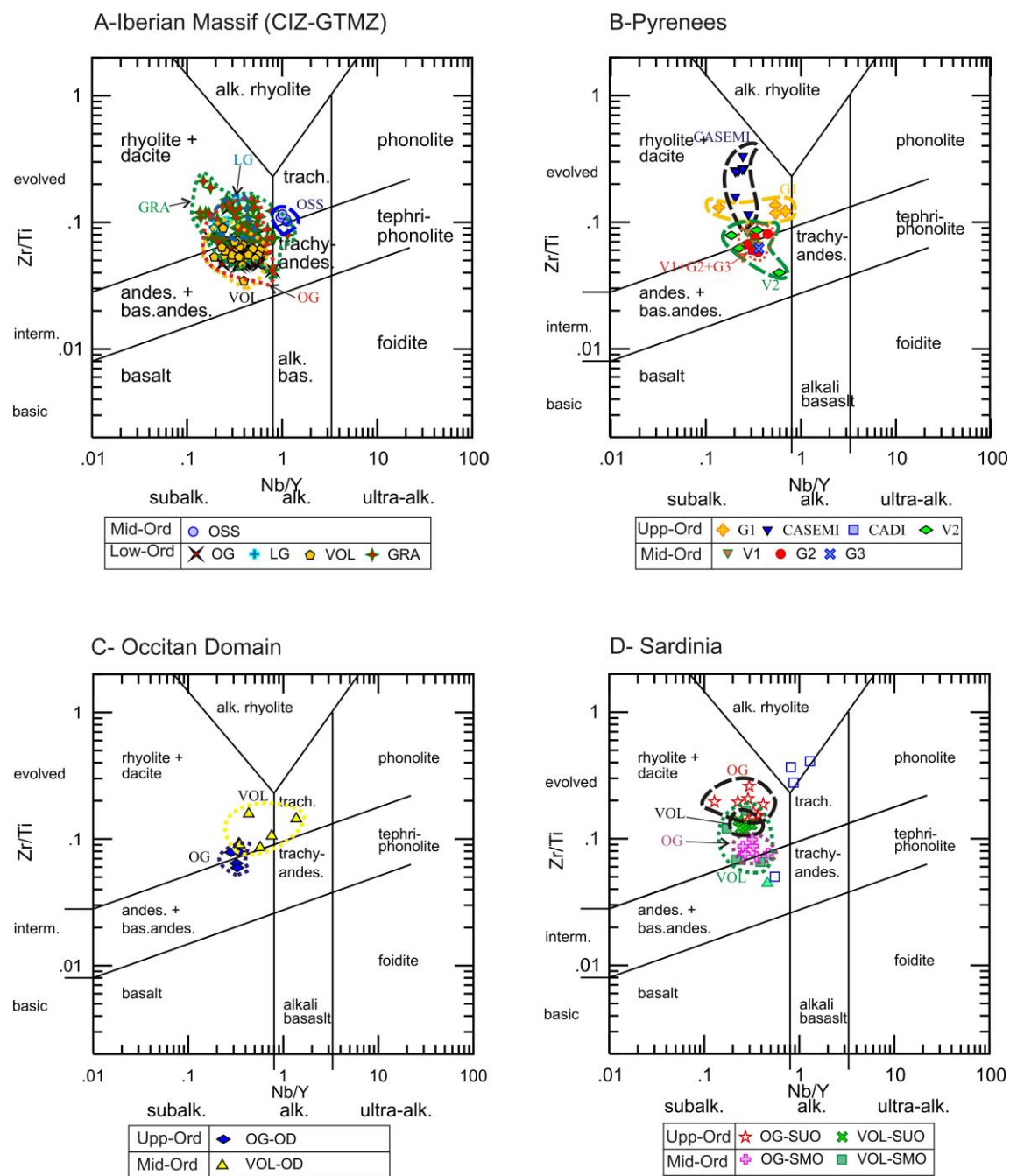


1607

1608

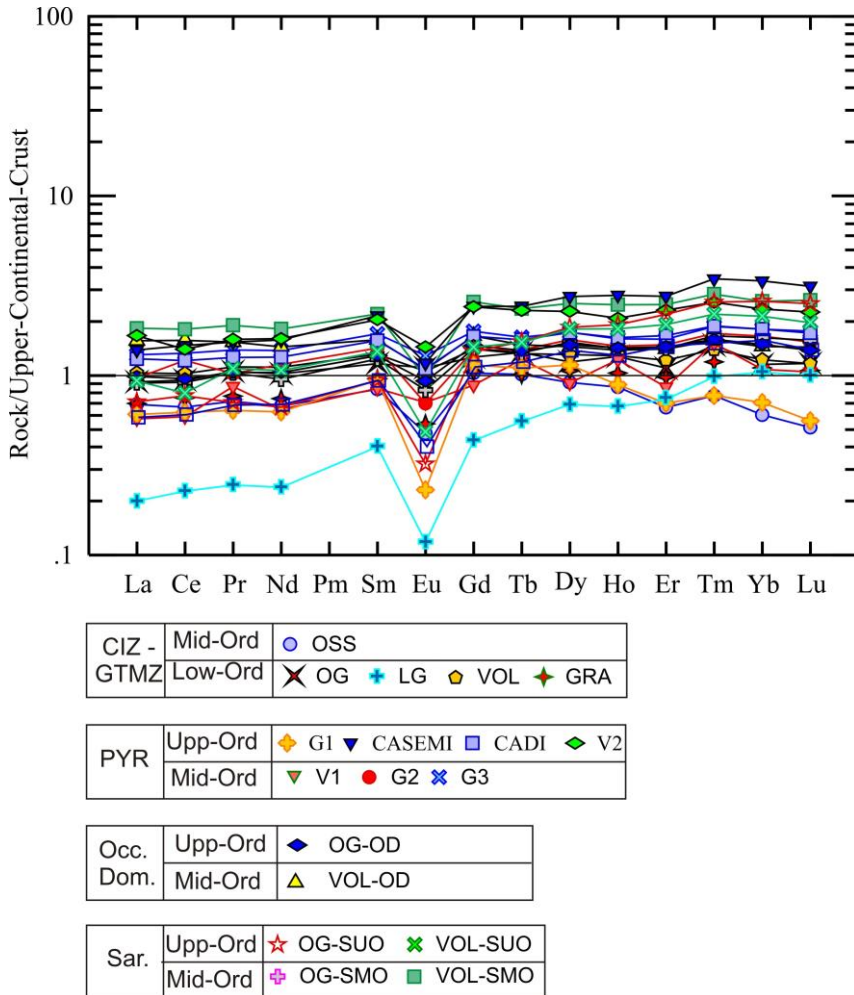
1609 **Figure 5.** Zr/Ti vs. Nb/Y discrimination diagram (after Winchester and Floyd, 1977;
 1610 Pearce, 1996). A. Lower–Middle Ordovician rocks of Iberian Massif (Central Iberian
 1611 and Galicia-Trás-os-Montes zones). B. Middle–Upper Ordovician rocks of the eastern
 1612 Pyrenees. C) Middle Ordovician rocks of the Occitan Domain. C–D. Middle–Upper
 1613 Ordovician rocks of Sardinia.

1614



1615

1616 **Figure 6.** Upper Crustal-normalized REE patterns (Rudnick and Gao, 2003) with
 1617 average values for all distinguished groups; symbols as in Figure 4.
 1618

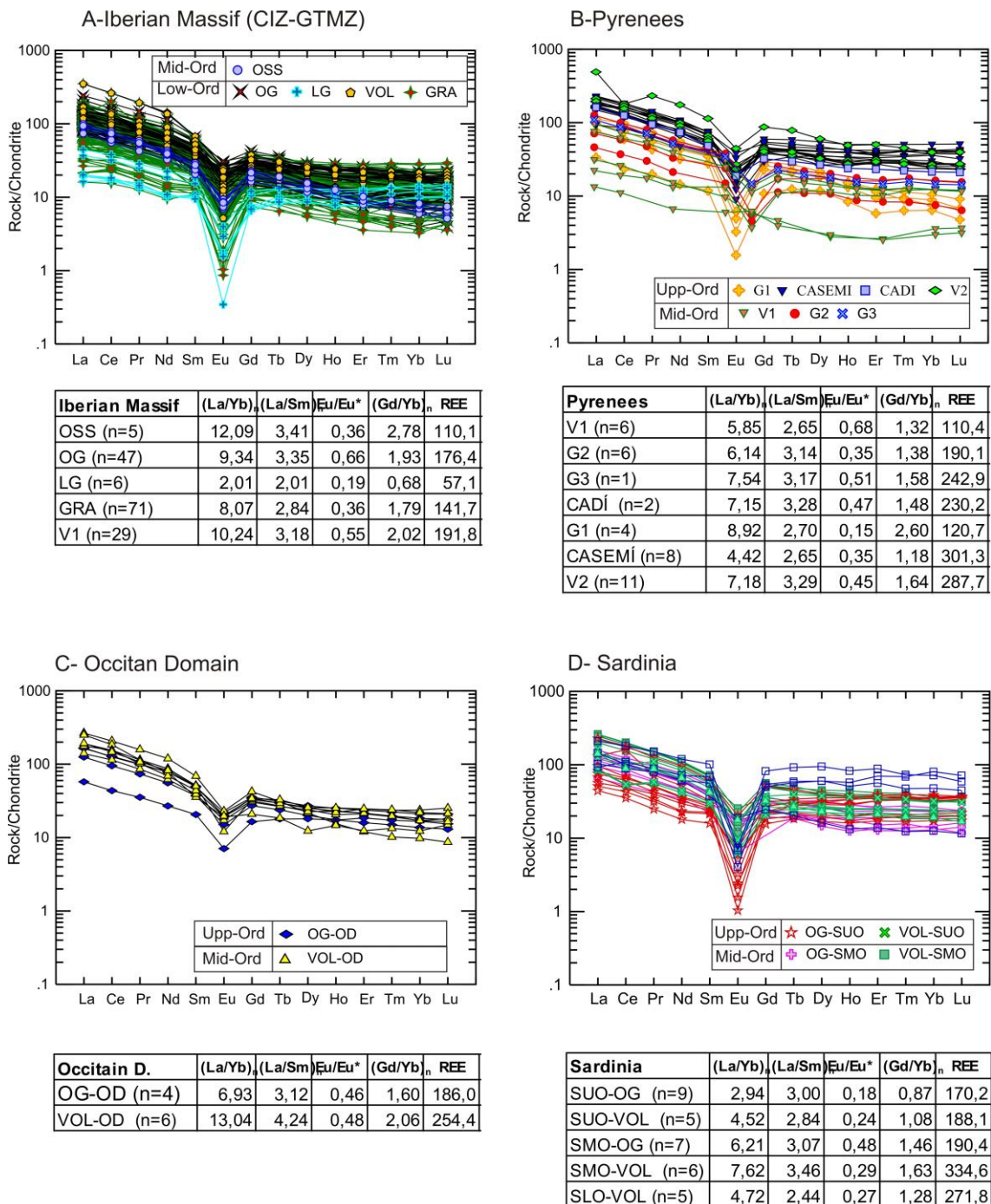


1619

1620

1621 **Figure 7.** Chondrite-normalized REE patterns (Sun and McDonough, 1989) for all
 1622 study samples.

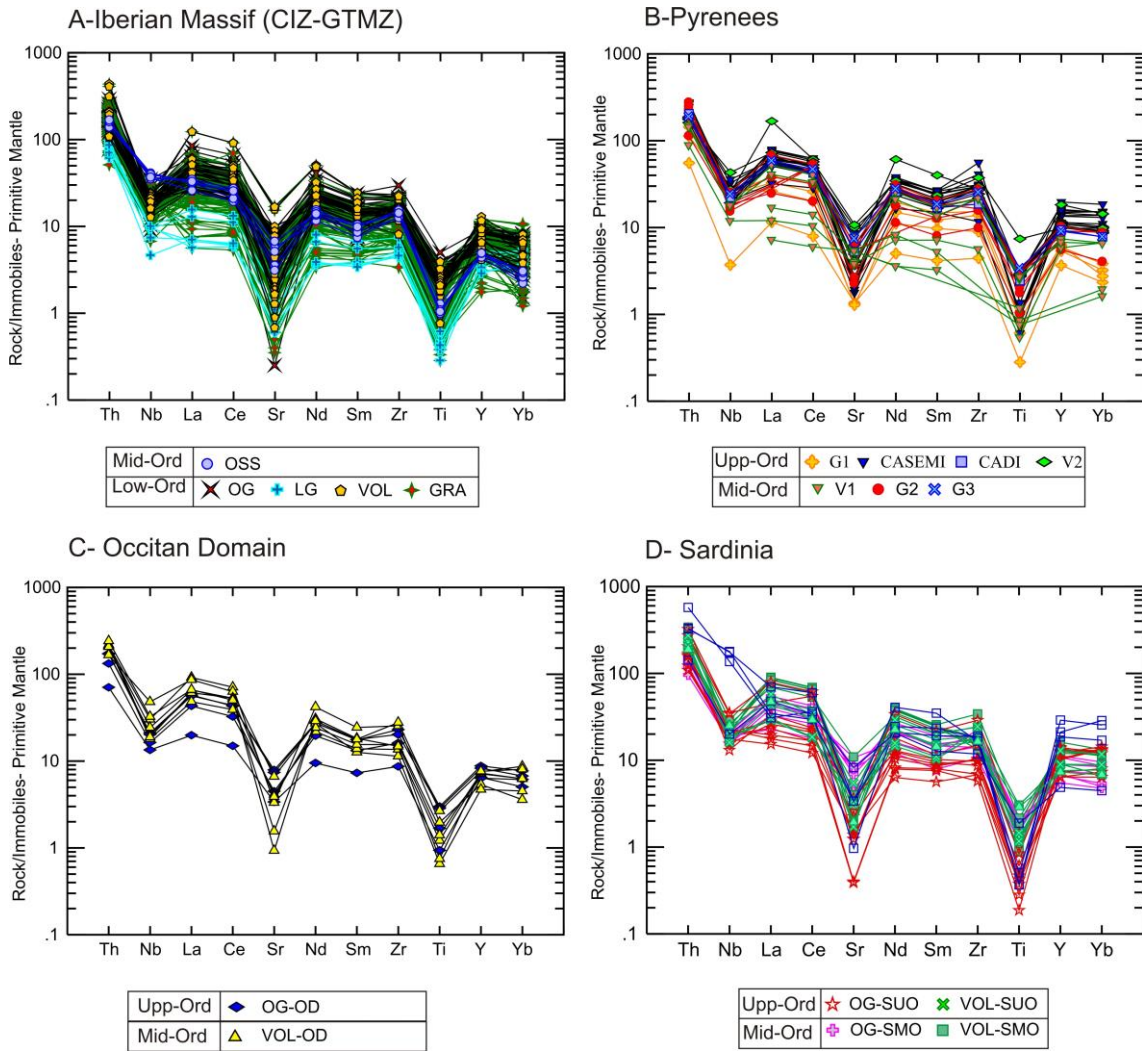
1623



1624

1625

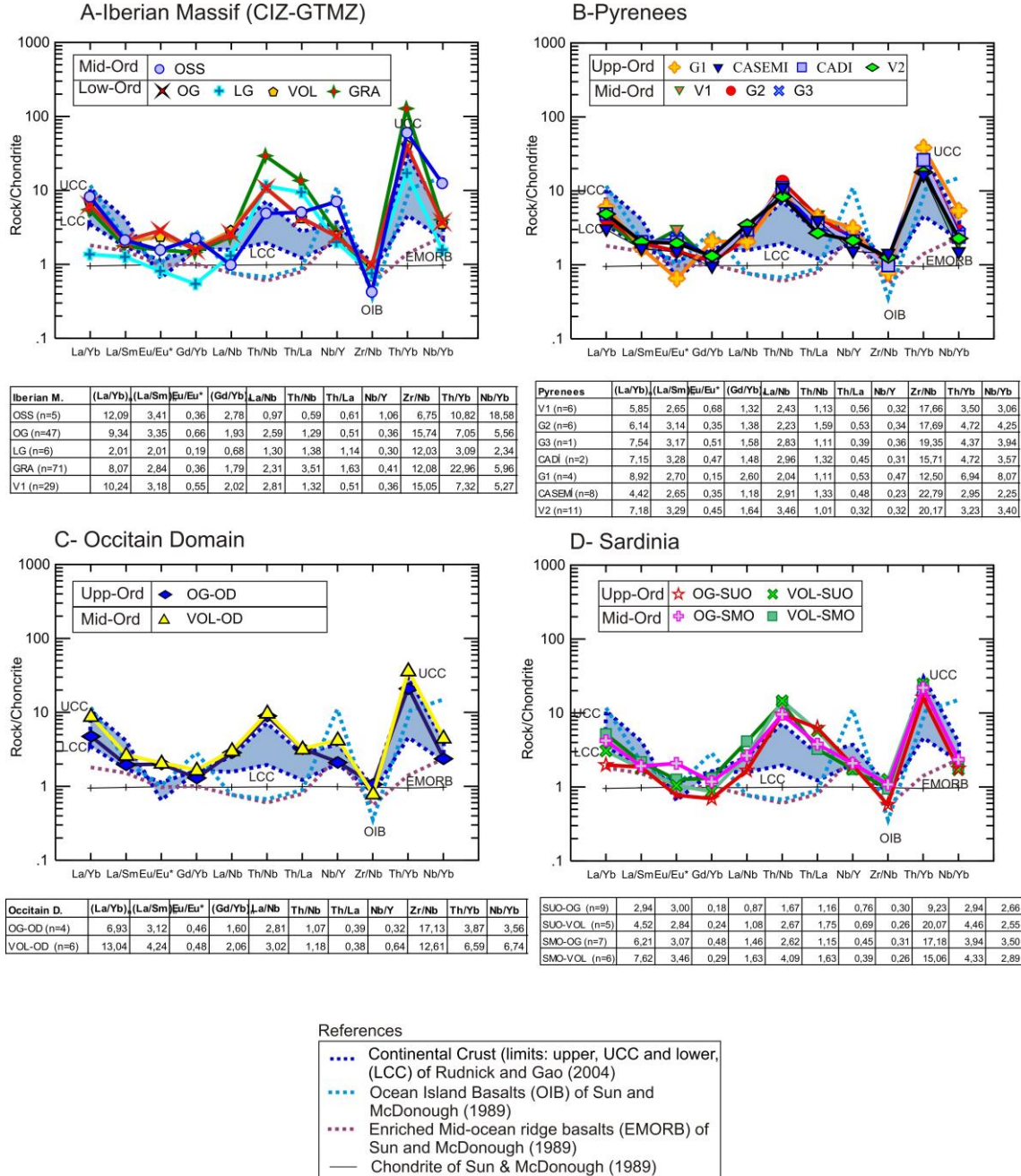
1626 **Figure 8.** Multi-element diagram normalised to Primitive Mantle of Palme and O'Neill
 1627 (2004) for all study samples.
 1628



1629

1630

1631 **Figure 9.** Chondrite-normalised isotope ratio patterns (Sun and McDonough, 1989) for
 1632 standard comparison for all study samples. Blue area: limits of continental crustal
 1633 values (Lower and Upper) of Rudnick and Gao (2003).
 1634

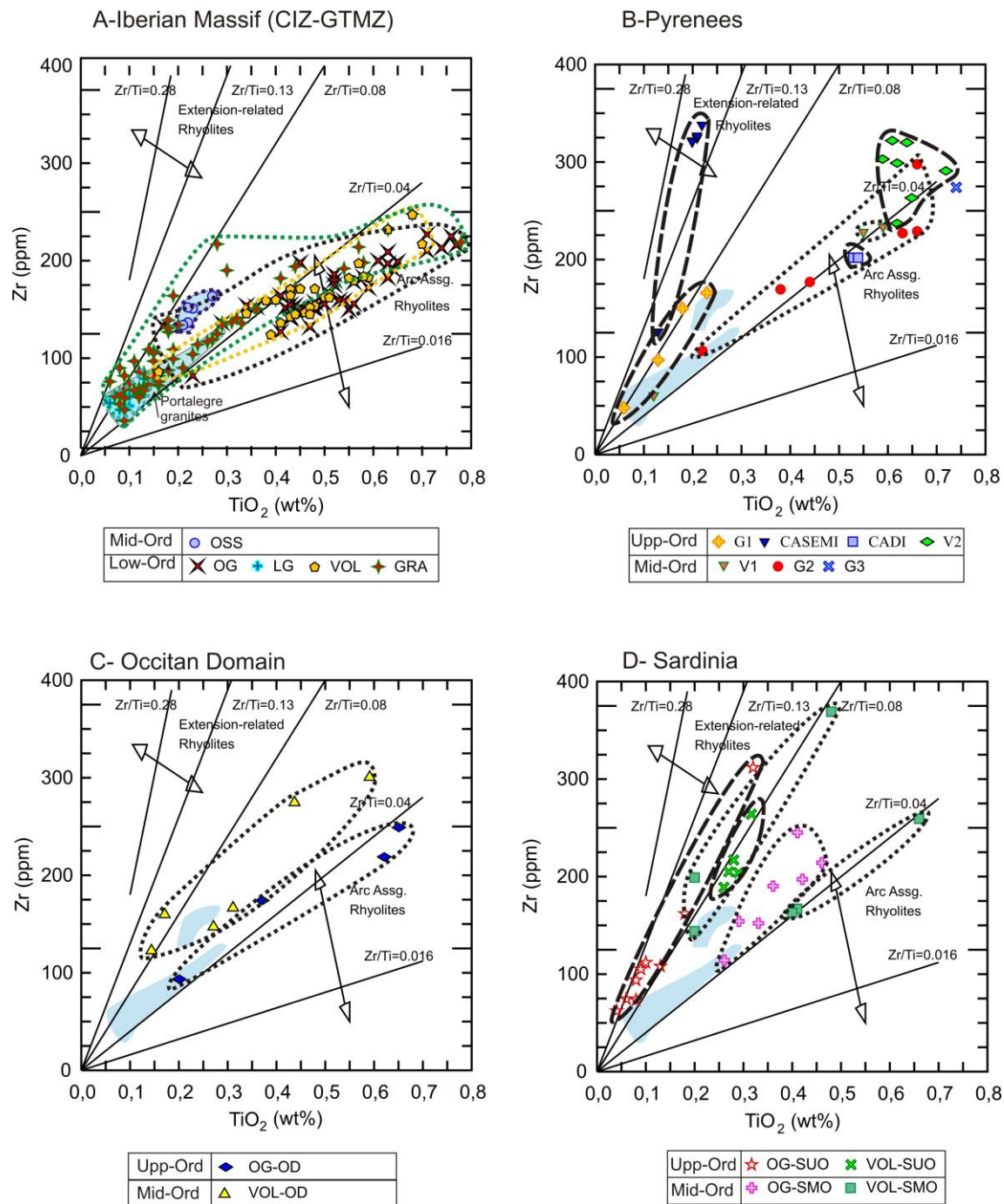


1635

1636

1637 **Figure 10.** Tectonic discriminating diagram of Zr vs. TiO_2 (Syme, 1998) for all study
 1638 samples. Double-sided arrows indicate ranging of different fields: rhyolites in tholeiitic
 1639 and calc-alkaline arc suites have Zr/ TiO_2 ratios ranging from about 0.016 to 0.04, and
 1640 extension-related rhyolites from about 0.13 to 0.28 (Syme, 1989).

1641

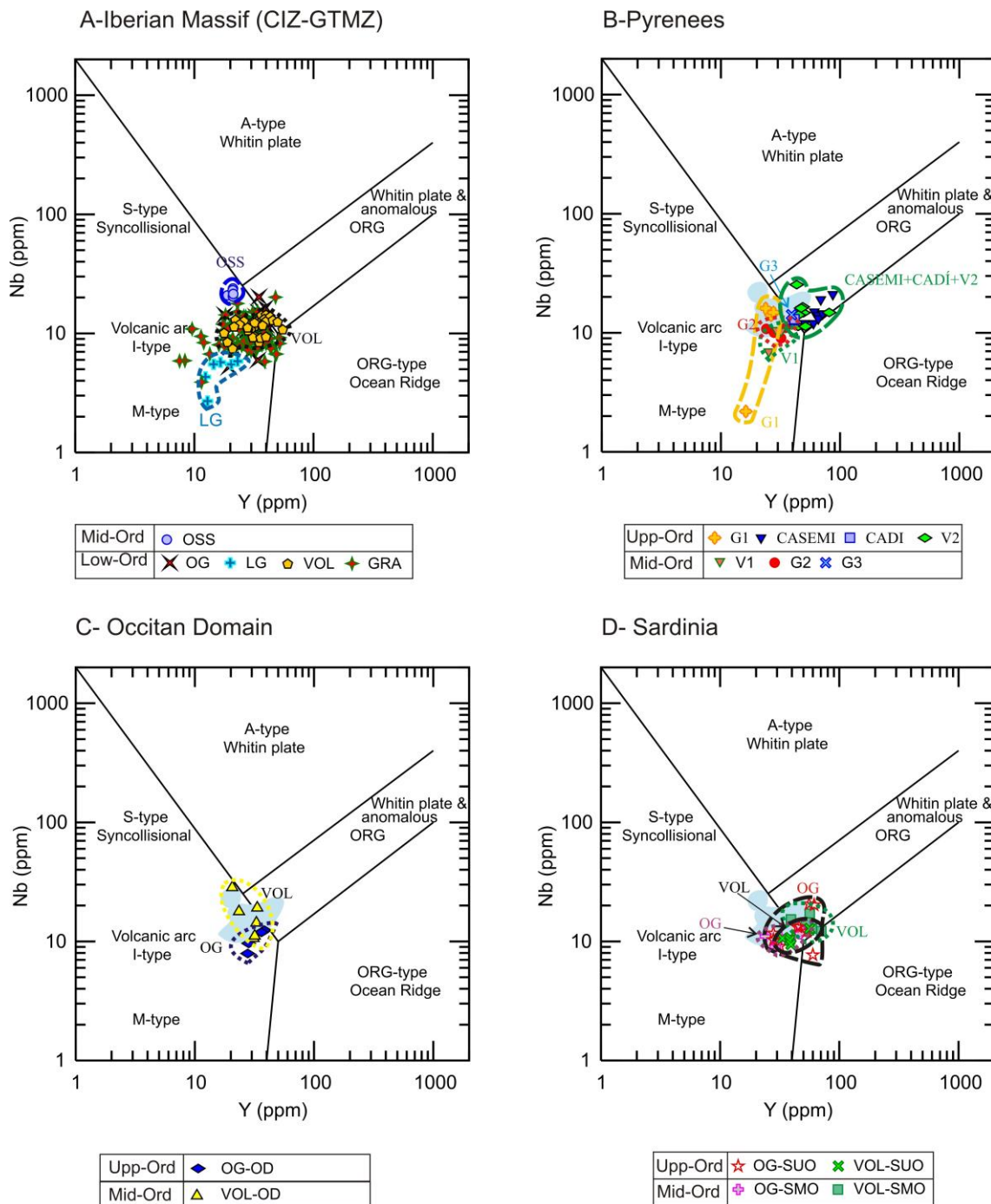


1642

1643

1644 **Figure 11.** Tectonic discriminating diagram of Y vs. Nb (Pearce et al., 1984) for all
 1645 study samples.

1646

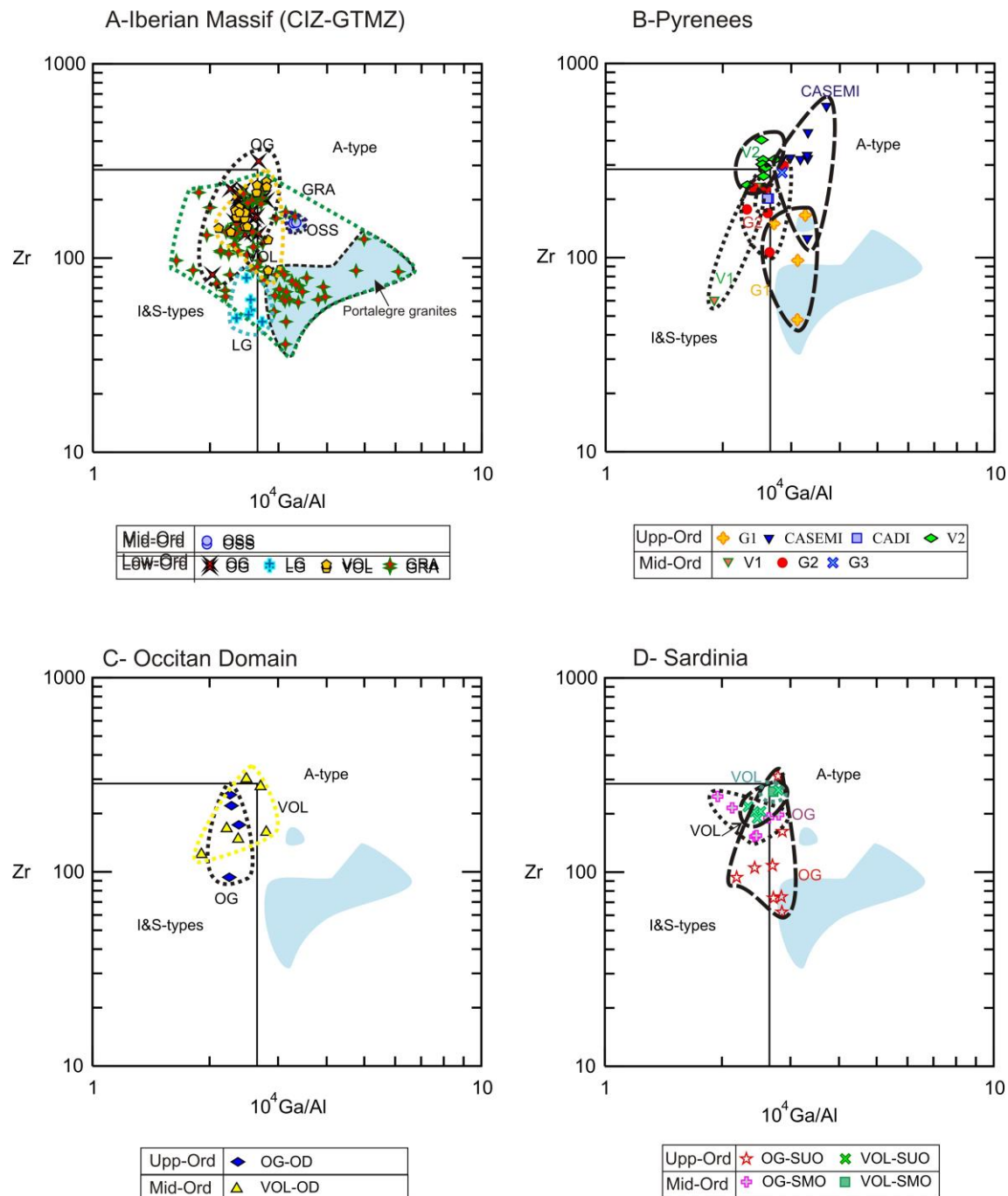


1647

1648

1649 **Figure 12.** Zr vs. 10^4 Ga/Al discrimination diagram (Whalen et al., 1987).

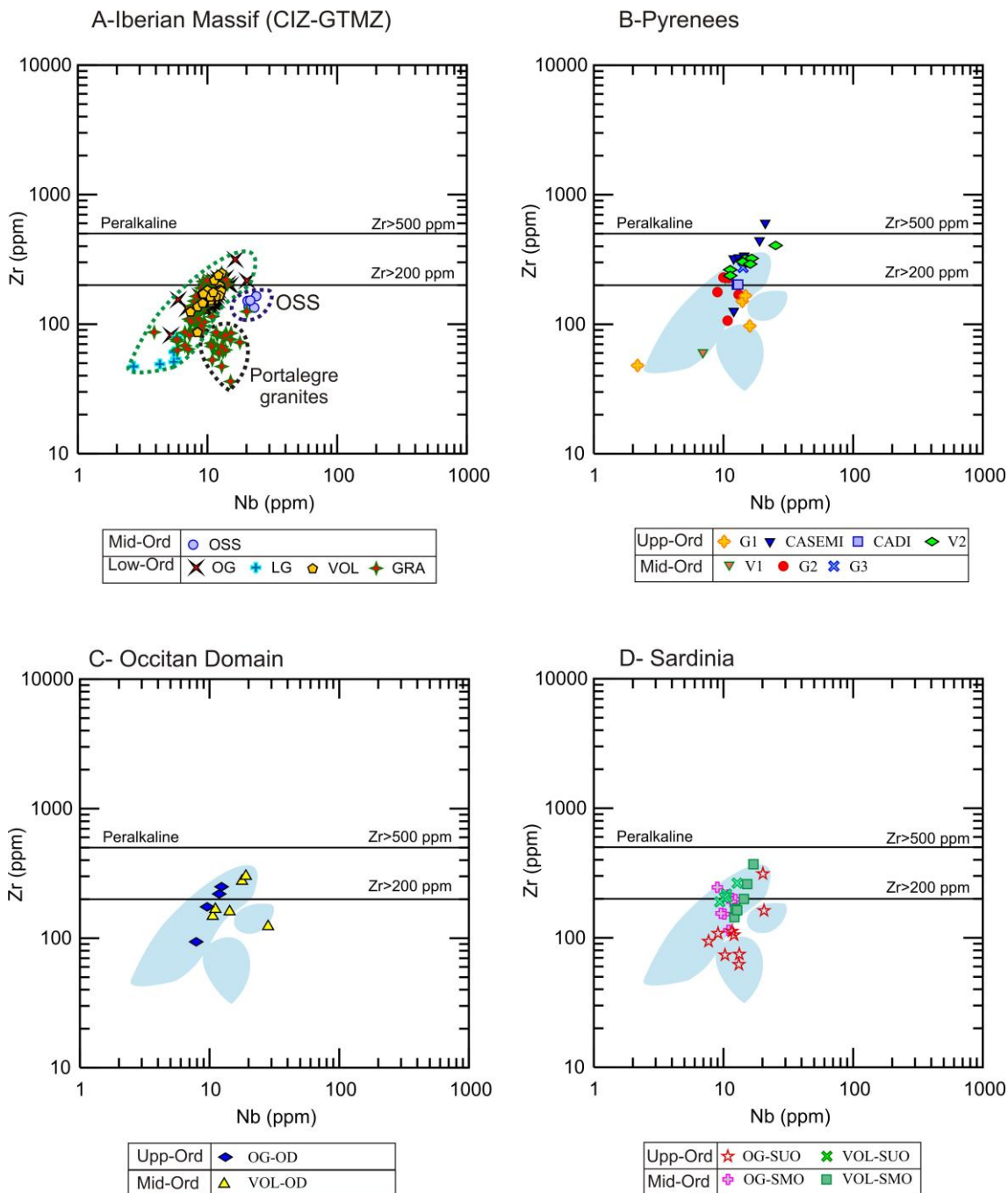
1650



1651

1652

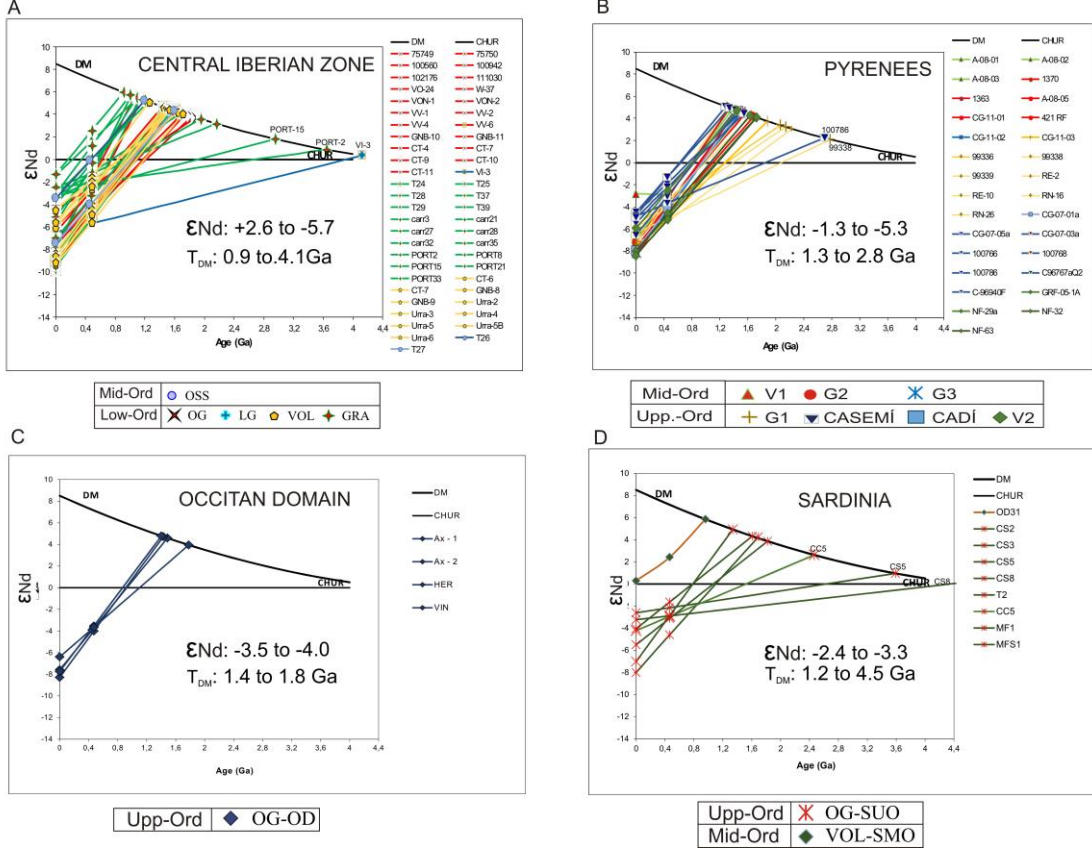
1653 **Figure 13.** Zr–Nb plot diagram (Leat et al., 1986; modified by Piercy, 2011) for all
 1654 study samples.
 1655



1656

1657

Figure 14. $\epsilon_{\text{Nd}}(t)$ vs. age diagram (DePaolo and Wasserburg, 1976; DePaolo, 1981) for study sampled. A. Central Iberian and Galicia-Trás-os-Montes Zones. B. Eastern Pyrenees. C. Occitan Domain. D. Sardinia; see references in the text.



1662

1663

1664 **Table 1.** Chemical analyses of magmatic rocks. ICP and ICP-MS methods at ACME–
 1665 LABS in Canada.

1666

Sample	PYRENEES			MONTAGNE NOIRE			SARDINIA									Inner Zone	
	Albera	Pallaresa	Andorra	Axial Zone			External Zone						Inner Zone				
				Ax - 1	Ax - 2	HER	VIN	CC 5	CS 2	CS 3	CS 5	CS 8	MF 1	MFS 1	T 2	PB50	PB100
Long. (E)	3°7'39"	1°27'43"	1°33'29"	2°13'50"	2°33'58"	2°57'58"	2°13'50"	8°50'37"	8°50'35"	8°50'35"	8°50'40"	8°50'35"	8°50'47"	8°52'02"	8°48'54"	9°09'32"	9°09'32"
Lat. (N)	42°25'2"	42°36'1"	42°32'30"	43°34'32"	43°29'3"	43°34'32"	43°17'45"	38°54'16"	38°52'38"	38°52'38"	38°52'36"	38°52'39"	38°54'58"	38°53'57"	38°53'57"	41°11"	41°11'04"
SiO ₂	68.38	71.67	69.18	70.38	67.43	68.31	73.97	76.43	75.14	76.52	76.61	76.36	72.13	75.94	75.55	68.93	67.24
TiO ₂	0.57	0.63	0.61	0.36	0.64	0.61	0.20	0.08	0.08	0.09	0.04	0.06	0.31	0.13	0.18	0.41	0.46
Al ₂ O ₃	15.68	14.24	15.05	14.90	15.76	15.39	13.82	13.28	12.81	11.80	12.71	12.63	13.80	13.16	12.94	16.32	15.79
Fe ₂ O ₃	4.09	4.54	4.20	3.04	4.11	4.19	2.05	0.69	1.39	1.44	1.28	1.35	2.96	1.55	1.62	3.19	4.78
MnO	0.07	0.06	0.05	0.04	0.04	0.04	0.04	0.01	0.01	0.01	0.01	0.01	0.02	0.03	0.04	0.08	0.08
MgO	1.35	0.78	1.16	0.78	1.33	1.34	0.43	0.08	0.15	0.16	0.06	0.05	0.36	0.19	0.08	1.15	1.58
CaO	0.21	0.53	1.78	1.22	1.44	1.58	0.62	0.32	0.25	0.15	0.20	0.35	0.61	0.38	0.17	3.05	2.70
Na ₂ O	4.07	1.67	3.40	3.33	2.78	2.93	2.87	3.04	1.71	1.58	2.91	3.35	2.89	2.57	2.53	3.85	3.43
K ₂ O	2.84	2.91	2.71	4.35	4.68	4.03	4.55	4.79	7.84	7.43	5.16	4.91	5.47	4.94	5.36	2.26	2.96
P ₂ O ₅	0.17	0.24	0.20	0.21	0.2	0.19	0.18	0.15	0.05	0.05	0.03	0.04	0.12	0.11	0.07	0.15	0.14
L.O.I.	2.03	2.60	1.50	1.2	1.3	1.2	1.2	1.1	0.4	0.7	0.9	0.8	1.1	0.9	1.4	0.90	0.70
Total	99.05	99.42	99.42	99.51	99.30	99.39	99.73	99.90	99.69	99.79	99.78	99.47	99.75	99.78	99.97	99.37	
As	77.20	1.70	6.80	2.50	6.00	1.80	1.90	0.70	1.00	0.50	2.80	1.10	1.80	101.10	4.00	5.00	5.00
Ba	742.50	388.00	398.00	499	1050	767	256	60	467	109	21	27	784	194	192	689.00	600.00
Be	2.44	3.00	2.00	4.00	2.00	5.00	3.00	6.00	3.00	1.00	9.00	2.00	7.00	3.00	7.00	3.00	5.00
Bi	0.30	0.20	0.10	0.20	0.20	0.20	0.40	0.30	0.10	0.10	0.10	0.10	0.10	0.70	0.40	4.00	4.00
Cd	0.18	0.10	0.10	0.10	0.10	0.10	0.10	0.10	0.10	0.10	0.10	0.10	0.10	0.10	0.10	0.10	0.10
Co	5.84	4.60	6.20	5.20	5.20	5.40	2.70	0.50	1.60	1.00	0.80	0.60	2.30	1.50	1.20	5.00	14.00
Cs	9.79	5.60	4.90	14.30	7.10	6.80	7.30	4.20	3.40	1.60	4.50	4.60	6.40	3.90	4.10	4.20	9.40
Cu	16.34	13.20	10.30	7.20	7.40	10.10	8.70	4.70	4.60	8.20	26.80	2.50	5.00	5.50	5.00	10.00	60.00
Ga	21.03	19.80	18.80	19.10	19.20	18.90	16.70	19.30	14.90	15.30	19.40	19.20	20.70	19.00	19.90	17.00	18.00
Hf	6.40	7.30	6.40	5.00	6.90	5.70	3.10	3.10	4.10	4.30	3.50	3.80	8.80	3.70	5.80	5.90	5.30
Mo	1.20	0.90	1.00	0.60	0.90	0.60	0.30	0.70	0.70	0.70	0.80	0.50	1.70	0.80	1.60	2.00	2.00
Nb	10.49	11.30	11.30	9.60	12.40	11.90	7.90	10.30	7.70	12.10	13.20	13.30	20.20	9.10	20.60	9.00	11.00
Ni	16.56	8.00	7.70	20.00	20.00	20.00	20.00	20.00	20.00	20.00	20.00	20.00	20.00	20.00	20.00	20.00	80.00
Pb	7.94	9.80	22.90	3.50	4.60	5.10	3.60	2.90	7.40	8.60	4.50	5.50	5.10	6.30	5.50	21.00	24.00
Rb	124.40	123.70	137.20	204.6	161.6	142.2	188.2	289.9	206.1	187.4	294.1	275.1	208.7	256.4	227.1	85.00	118.00
Sb	2.27	0.10	0.30	0.10	0.10	0.10	0.10	0.10	0.10	0.10	0.10	0.10	0.10	0.10	0.10	5.00	5.00
Sc	10.00	10.00	6.00	9.00	9.00	4.00	4.00	3.00	3.00	4.00	4.00	4.00	15.00	4.00	8.00	9.00	12.00
Sn	2.11	5.00	5.00	9.00	3.00	3.00	7.00	9.00	4.00	3.00	13.00	15.00	7.00	15.00	12.00	3.00	3.00
Sr	158.00	201.80	83.70	91.20	160.30	150.10	68.70	30.70	73.90	25.20	7.90	8.10	59.90	45.60	25.00	217.00	167.00
Ta	1.07	1.10	1.10	0.80	1.00	0.80	0.70	2.10	0.90	1.10	3.40	1.70	1.60	1.70	2.30	1.00	1.20
Th	11.90	15.70	13.50	11.10	14.40	14.30	5.90	9.10	14.10	17.00	13.50	13.10	22.80	10.20	26.90	13.30	11.50
U	3.70	5.10	4.60	4.10	3.60	3.20	4.80	3.30	2.90	3.20	3.50	3.50	4.60	8.10	4.90	4.50	2.20
V	44.49	49.00	36.00	36.00	63.00	68.00	22.00	8.00	8.00	8.00	8.00	8.00	15.00	8.00	10.00	62.00	53.00
W	1.80	1.90	2.50	3.20	2.60	1.60	3.00	5.60	0.90	2.10	5.20	3.00	2.40	4.40	3.50	1.00	20.00
Y	29.29	43.90	50.60	28.30	38.40	36.20	27.80	28.00	60.10	53.60	44.40	46.00	61.60	31.80	55.80	29.00	24.00
Zn	63.71	52.00	70.00	55.00	71.00	78.00	46.00	7.00	35.00	39.00	15.00	24.00	37.00	30.00	22.00	70.00	70.00
Zr	233.30	263.20	237.10	174.40	249.20	219.10	93.70	73.50	93.80	105.10	62.20	74.50	311.80	108.10	161.90	245.00	214.00
La	27.90	45.30	38.00	29.60	39.50	38.70	13.60	10.50	22.70	19.50	12.10	13.40	54.20	17.90	31.30	26.90	34.30
Ce	59.00	86.90	75.50	58.10	77.00	78.20	26.70	21.60	42.10	39.70	26.20	29.90	109.80	37.40	97.60	53.20	70.50
Pr	7.26	9.80	8.47	6.99	9.41	9.55	3.36	2.36	4.73	4.85	3.00	3.24	11.94	4.07	6.86	5.88	8.20
Nd	27.83	35.60	31.20	26.00	36.40	36.40	12.60	8.40	16.60	17.10	10.50	10.90	44.70	15.00	24.00	21.60	29.40
Sm	5.80	7.69	7.16	5.70	7.55	7.63	3.15	2.43	4.10	4.41	3.28	3.44	9.37	3.88	4.93	4.70	6.00
Eu	0.98	1.05	1.03	0.87	1.27	1.15	0.41	0.14	0.43	0.13	0.06	0.09	1.17	0.30	0.19	0.95	0.93
Gd	5.22	8.32	7.89	5.59	7.28	7.05	3.38	3.20	5.60	5.50	4.42	4.69	10.60	4.50	6.34	4.00	5.10
Tb	0.87	1.26	1.27	0.89	1.17	1.10	0.67	0.69	1.13	1.18	1.03	1.07	1.70	0.82	1.27	0.70	0.80
Dy	5.30	6.68	8.00	5.09	6.89	6.39	4.59	4.30	7.69	8.23	7.31	7.66	10.28	5.24	9.00	3.70	4.30
Ho	1.06	1.52	1.73	0.99	1.42	1.30	0.98	0.91	1.91	1.91	1.59	1.65	2.13	1.12	2.01	0.70	0.80
Er	2.98	4.52	4.96	2.64	3.92	3.56	3.07	2.85	5.80	6.46	5.35	5.38	6.25	3.64	6.17	2.20	2.10
Tm	0.46	0.60	0.73	0.38	0.57	0.50	0.44	0.43	0.91	1.00	0.85	0.85	0.89	0.52	0.92	0.35	0.32
Yb	3.00	3.98	4.72	2.33	3.56	3.11	2.83	2.95	5.81	6.60	6.10	6.16	5.53	3.70	6.04	2.50	2.20
Lu	0.44	0.58	0.69	0.33	0.53	0.45	0.39	0.44	0.90	0.94	0.92	0.94	0.86	0.56	0.90	0.41	0.36

1667

1668

1669 **Table 2.** Summarized geochemical features of the Furongian and Ordovician felsic
1670 episodes described in the text; data from Lancelot et al. (1985), Calvet et al. (1988),
1671 Valverde-Vaquero and Dunning (2000), Roger et al. (2004), Vilà et al. (2005),
1672 Giacomini et al. (2006), Díez-Montes (2007), Montero et al. (2007, 2009), Solá (2007),
1673 Zeck et al. (2007), Castiñeiras et al. (2008b), Talavera (2009), Casas et al. (2010),
1674 Navidad et al. (2010, 2018), Liesa et al. (2011), Martínez et al. (2011, 2018), Navidad
1675 and Castiñeiras (2011), Gaggero et al. (2012), Talavera et al. (2013), Villaseca et al.
1676 (2016), Pouclet et al. (2017), Cruciani et al. (2018) and this work. Abbreviations: C/Z
1677 Central Iberian Zone, GTOMZ Galicia-Trás-os-Montes Zone, OCC Occitan Domain,
1678 PYR Pyrenees and SAR Sardinia; * *sensu* Guitard (1970); A/CNK ratio is always
1679 peraluminous.

ORTHOGNEISS FACIES	code	composition	SiO ₂ wt. %	Na ₂ O wt. %	K ₂ O wt. %	Al/CNK ratio	End	TDM (Ga)	¹⁴⁷ Sm/ ¹⁴⁴ Nd area
(1) Furlongan-Mid Ordovician Suite									
CIZ - Olio de Sapo orthogneiss	OG	K-rich dacite to rhyolite	75-60.3	3.9-0.1	5.9-3.4	3.1-1.0	-5.1 to -1.8	1.8-1.1	0.15-0.09 Sanabria (ca. 472 Ma) and Guadarrama (ca. 488-473 Ma)
CIZ - Leucogneiss	LG	K-rich dacite to rhyolite	75.9-73.6	3.1-2.7	5.3-4.2	1.3-1.1	-5.1 to -4.9	4.1	0.22-0.18 Guadarrama
CIZ - Metagranite	GRA	K-rich dacite to rhyolite	77-64.6	4.8-0.5	6.3-2.5	1.8-1.0	-5.2 to +2.6	3.6-0.9	0.19-0.09 NE Central System, Sanabria, Miranda do Douro (ca. 496-473 Ma), CZ (496-471 Ma) for Carascal, Fermoselle, Ledesma, Portalegre and Viljudino granites)
CIZ/GTMZ - Volcanic rocks	VOL.	andesite to rhyolite	79.3-64.6	3.2-0.1	6.3-2.2	2.7-1.1	-5.5 to -1.6	1.7-1.3	0.15-0.13 Saldanha Fm. in GTMZ, Olio de Sapo Fm. in Sanabria, and Urria Fm.
CIZ - San Sebastián orthogneiss	OS	rhyolite	75.4-73.8	3.1-2.5	5.4-4.9	1.2-1.1	-4.0 to 0	1.6-1.2	0.14-0.14 Sanabria (ca. 470-465 Ma)
PYR - augengneiss	G2*	dacite to rhyolite	73.6-68.3	3.9-3.2	4.4-2.5	1.2-1.1	-4.4 to -3.0	1.4-1.2	0.14-0.13 c. 476-462 Ma
PYR - orthogneiss	G3*	K-rich dacite	73.5-68.4	2.9-2.4	4.4	1.2	-4.2	1.33	0.13 c. 463 Ma
PYR - volcanic rocks	V1	Na-rich rhyolite	73.5-68.4	7.8-2.4	3.2-1.3	2.0-1.1	-5.1 to -2.6	1.7-1.6	0.19-0.13 Pierrefitte Fm. and Albera massif (ca. 472-465 Ma)
OCC - volcanic rocks	VOL-OD	K-rich dacite to rhyolite	75.6-66.7	3.7-0.6	9.3-2.3	2.4-1.3			Saint-Sémin-sur-Rance and Saint-Salvi-de-Carcavés nappes
SAR - orthogneiss	OG-SMO	K-rich rhyolite	74-67.2	3.8-2.6	5.8-2.3	1.3-1.1			c. 469 Ma
SAR - volcanic rocks	VOL-SMO	K-rich dacite to rhyolite	76.7-67.6	4.7-1.9	5.4-2.9	2.0-1.2			0.16 c. 464-462 Ma
(2) Upper Ordovician Suite									
PYR - orthogneiss	G1*	K-rich dacite to rhyodacite	76.4-73.4	3.1-2.6	5.3-4.7	1.2-1.1	-5.3 to -3.1	2.7-1.5	0.17-0.12 c. 457 Ma
PYR - orthogneiss	CADI	K-rich dacite to rhyodacite	69.4	3	4	1.2	-4.1	1.5	0.13 Cadi massif (ca. 456 Ma)
PYR - orthogneiss	CASEMI	K-rich dacite to rhyodacite	76-71.9	4-1.8	6.3-3.2	1.2-0.9	-3.6 to -1.3	2.6-1.3	0.17-0.13 Casemi massif (ca. 451-446)
PYR - volcanic rocks	V2	andesite to rhyodacite	86.1-63	6-0	4.3-0.6	3.6-1	-5.1 to -2.6	1.7-1.6	0.14-0.14 Ribes de Freser, Andorra (ca. 457 Ma), Pallaresa (ca. 453 Ma), Els Meigs (ca. 455.2 Ma)
OCC - orthogneiss	OG-OD	K-rich dacite to rhyolite	73.9-67.4	3.3-2.8	4.7-4	1.3-1.2	-4 to -3.5	1.8-1.4	0.15-0.13 Gorges d'Héric (ca. 450 Ma; Caroux), S. Mazanet (None), S. Rouairoux (Agout), Le Vintrou
SAR - External Zone orthogneiss	OG-SUD	K-rich dacite to rhyolite	76.8-72.1	3.3-1.6	7.8-4.8	1.3-1.1	-3.3 to -1.6	4.2-1.2	0.19-0.12 Capo Spartivento, Cuille Culurgion, Tuerredda, Monte Filau, Monte Sestiballas (ca. 458-457 Ma)
SAR - Nanpe 3' zone volcanic rocks	VOL-SUD	K-rich dacite to rhyodacite	76.7-70.7	3.3-1.6	7.8-4.8	1.3-1.1			Trizzulla Fm. at Monte Grindini